

A Discrete Variational Approach for Investigation of Stationary Localized States In A Discrete Nonlinear Schrödinger Equation, Named IN-DNLS

K. Kundu

Institute of Physics, Bhubaneswar 751005, Orissa, India.

(Dated: November 21, 2018)

IN-DNLS, considered here is a countable infinite set of coupled one dimensional nonlinear ordinary differential difference equations with a tunable nonlinearity parameter, ν . This equation is continuous in time and discrete in space with lattice translational invariance and has global gauge invariance. When $\nu = 0$, it reduces to the famous integrable Ablowitz - Ladik (AL) equation. Otherwise it is nonintegrable. The formation of unstaggered and staggered stationary localized states (SLS) in IN-DNLS is studied here using discrete variational method. The appropriate functional is derived and its equivalence to the effective Lagrangian is established. From the physical consideration, the ansatz of SLS is assumed to have the functional form of stationary soliton of AL equation. So, the ansatz contains three optimizable parameters, defining width (β^{-1}), maximum amplitude and its position ($\sqrt{\Psi}$, x_0). Four possible situations are considered. An unstaggered SLS can be either on-site peaked ($x_0 = 0.0$) or inter-site peaked ($x_0 = 0.5$). On the other hand, a staggered SLS can be either Sievers-Takeno (ST) like mode ($x_0 = 0.0$), or Page(P) like mode ($x_0 = 0.5$). It is shown here that unstable SLS arises due to incomplete consideration of the problem. In the exact calculation, there exists no unstable mode. The width of an unstaggered SLS of either type decreases with increasing $\nu > 0$. Furthermore, on-site peaked state is found to be energetically stable. These results are explained using the effective mass picture. For the staggered SLS, the existence of ST like mode and P like mode is shown to be a fundamental property of a system, described by IN-DNLS. Their properties are also investigated. For large width and small amplitude SLS, the known asymptotic result for the amplitude is obtained. Further scope and possible extensions of this work are discussed.

PACS numbers: 05.45.Yv, 45.10.Db, 45.Jj, 52.35.Mw, 63.20.Pw, 63.20.Ry

I. INTRODUCTION

The study of energy localization in nonlinear lattices has become an important field of research in nonlinear dynamics in the past couple of decades[1]. In this context, the subject of intrinsic localized modes (ILM) has drawn a considerable attention as it offers appealing insights into a variety of problems ranging from the non-exponential energy relaxation[2] in solids, to the local denaturation of DNA double strands[3]. The subject is also an intense field of study in material science, and nonlinear optic applications[4, 5].

The necessary condition for the formation of intrinsic localized modes (ILMs) or excitations in translationally invariant nonlinear systems is the balance between nonlinearity and dispersion. Furthermore, by localized it is meant that the amplitude of such modes goes to zero at the boundaries of the system, which is taken to be infinitely large. In other words, the relevant localization length scale is much much smaller than the system size length scale. There are two broad classes of intrinsic localizations in $(1 + 1)$ dimensional nonlinear continuous systems[6]. Shape preserving localized excitations, arising in nonlinear continuous systems by satisfying the above mentioned balancing condition are called dynamical solitons[7, 8, 9]. Solitons in continuous nonlinear Schrödinger equation (cNLS) is an example of dynamical solitons[9, 10]. By solitons we usually mean moving shape preserving nonlinear excitations, though there can be stationary solitons also. Take for ex-

ample cNLS. One particular one-soliton solution of this equation is a stationary soliton[10]. Breathers belong to the second category of ILM in nonlinear systems[6]. Breathers are spatially localized time periodic solutions of nonlinear equations. They are characterized by internal oscillations[6, 7, 11, 12, 13, 14, 15, 16, 17, 18, 19, 20, 21, 22]. Again, by breathers we usually imply stationary localized excitations in nonlinear systems. However, under appropriate conditions, nonlinear systems may have moving breathers[7]. As for examples, we note that breathers can be found in continuous systems, described by sine-Gordon (sG) equation and modified KdV (mKdV) equation[7]. Even in cNLS, the stationary one-soliton solution is nothing but a breather[12]. So, the distinction between solitons and breathers is not always very rigorous. Breathers are, however rare objects in continuous nonlinear equations and are usually unstable[12]. It is important in the present context to note that continuous nonlinear equations may have Galilean or Lorentz invariance. For example, KdV and cNLS are Galilean invariant[7]. So, a soliton of some fixed amplitude in the cNLS and KdV can be Galileo boosted to any velocity. Similarly, sG equation has both stationary and moving breather solutions[7, 22]. These two solutions are, however, connected by Lorentz transformation[7]. So, in dealing with stationary ILMs, we consider that moving frame which is at rest with respect to the ILM.

However, models describing microscopic phenomenon in condensed matter physics are inherently discrete, with the lattice spacing between atomic sites being a fun-

damental physical parameter. For these systems, an accurate microscopic description involves a set of coupled ordinary differential-difference equations (ODDE). Coupled ODDEs are also encountered in the study of many important problems in optics and other branches of science[12, 22, 23]. So, it is pertinent to discuss next what features of continuous nonlinear equations are possibly destroyed and what novel features can arise from the discretization of at least one of the variables, say one spatial dimension.

In the general discrete case, Galilean or Lorentz invariance in relevant dynamical equations may not be present at all or may not be transparent at the equation level. Consider, for example the AL[24, 25] and the N-AL equations[26]. First one is the example of an integrable nonlinear differential discrete equation, which is often referred to as the integrable discretization of the cNLS equation. The other equation provides an example of a differential discrete nonintegrable nonlinear equation, having solitary wave solutions. Most importantly, the existence of solitary waves in the N-AL equation can be shown analytically[26]. The solitary wave solutions of these equations have continuous translational symmetry, which can be seen from the analytical expression of the one-soliton solution of the AL equation. This, in turn implies that both the AL and the N-AL equations have the Galilean invariance. So, also in case of ODDEs, stationarity in the ILM will imply the moving frame which is at rest with respect to the ILM.

The replacement of the spatial derivatives by spatial differences in the equation of motion implies the reduction of symmetry of the Hamiltonian, for systems executing Hamiltonian dynamics. In general, lowering the symmetry means enriching the class of solutions, because less restrictions are imposed. Of course, solutions are also lost by lowering the symmetry - namely ones which are generated by higher symmetry[12]. Let us consider in this context two discrete nonlinear equations, the Frenkel-Kontorova (FK)[22, 27] and the discrete nonlinear Schrödinger(DNLS) equations[28]. These are obtained by standard discretization of sG and cNLS respectively[22, 23, 28, 29]. The FK model can be used to describe a broad spectrum of nonlinear physically important phenomena, such as propagation of charge-density waves, the dynamics of adsorbed layer of atoms on crystal surfaces, commensurate-incommensurate phase transitions, domain walls in magnetically ordered structures etc[22, 27]. On the other hand, to name a few, DNLS has been used to model the self-trapping phenomenon in nonlinear waveguide arrays[23], to investigate a slow coherent transport of polarons in (1+1) dimension in condensed matter physics[28], and to study the dynamical phase diagram of dilute Bose-Einstein condensates[6]. We note that both of these discrete equations are nonintegrable while their continuous versions are integrable. It is relevant in this context to know that kink and antikink solutions of sG equation, which is the continuous integrable version of FK model are moving topological solitons, and

they arise due to the balance between nonlinearity and constraints originating from topological invariants in the system[9]. On the other hand, there exists no steady-state solutions for a moving kink in the FK model. What we obtain instead is static kinks[22]. To understand this, we note that the uniform discretization of space variables transforms continuous translational invariance to lattice translational invariance. This, in turn leads to a periodic arrangement of Peierls-Nabarro (PN) potential[22, 30]. Therefore, while the continuous translational invariance leads to zero frequency Goldstone modes in the system, discreteness introduces the PN barrier, with the barrier energy E_{PN} [22]. Due to this potential any moving kink radiates phonons and loses energy (E_{kink}). When $E_{kink} < E_{PN}$, the kink is trapped in one of the potential wells and further loss of energy by the kink by radiation of phonons takes it to the bottom of the well. This, in turn yields static kinks. Similarly, sG breathers arise due to the high symmetry of the equation, and consequently are unstable towards perturbation[12]. As the discreteness in space variables act as an external symmetry breaking perturbation, even a weak discreteness does not allow oscillating breather modes exist as dynamical eigenmodes of the sG chain, and breathers are destroyed by radiation of linear waves. In case of DNLS, similar analysis has been done in a perturbative frame using AL one-soliton solution as the zeroth order approximation[28, 31]. This analysis also shows that discreteness introduces a trapping potential for moving solitons and when discreteness exceeds a critical value, solitonic modes are trapped leading ultimately to pinned or stationary solitons.

It is already mentioned that the AL equation is an integrable discrete nonlinear equation. More specifically, the said equation is a countably infinite set of one dimensional nonlinear ordinary differential difference equations. This equation is continuous in time, but discrete in space with lattice translational invariance. The exact one-soliton solution of the AL equation is characterized by two parameters, namely, $\beta \in [0, \infty)$ and $k \in [-\pi, \pi]$ [24, 25]. For each β , there exists a band of velocities, determined by the other parameter, k , at which the soliton can travel without experiencing any PN pinning from the lattice discreteness[32]. Consider now other nonlinear equations in this series, namely the N-AL equation[26], the modified Salerno equation (MSE)[28, 33] and the IN-DNLS[32]. All these equations are nonintegrable extension of the AL equation, containing tunable nonlinearities. The N-AL equation is postulated and investigated to study the effect of dispersive imbalance on the maintenance of the moving solitonic profile. The importance of this equation lies in its appearance in the dynamics of vibrons and excitons in soft molecular chains[26, 28]. The solitary wave solutions of this equation are also characterized by the same two AL parameters, β and k . However, only certain values of k are allowed, though β can take all possible permissible values. At the allowed values of k , the term which imparts nonintegrability disappears. This, in turn makes

the solitary waves transparent to the PN potential, arising from the lattice discreteness. For other values of k , the initial AL one-soliton profiles are observed numerically to leave phonon tails behind, causing both slowing down and distortion of the initial profile. Important too in this context is an analytical investigation in a perturbative framework of the dynamics of a moving AL soliton, described by the N-AL equation. This analysis suggests that any moving soliton having energy below the PN barrier, induced by the discreteness in the lattice will be pinned, yielding thereby stationary solitons[26].

The IN-DNLS is a hybrid form of the AL equation and the DNLS, again with a tunable nonlinearity, the tuning of which switches the equation from the integrable AL equation to the nonintegrable DNLS[32]. To gauge the physical significance of this equation, we mention the followings. This equation is studied to investigate the discreteness induced oscillatory instabilities of dark solitons[34]. Furthermore, a discrete electrical lattice where the dynamics of modulated waves can be modeled by this equation is studied to investigate the modulation instability of plane waves[35]. In the MSE, the usual DNLS is replaced by a modified version of DNLS, the ADNLS, which involves acoustic phonons instead of optical phonons in condensed matter physics parlance[28, 31]. The study of this equation is also important in understanding the dynamics of vibrons and excitons in soft molecular chains. It is important to note that both IN-DNLS and MSE investigate the competition between the on-site trapping and the solitonic motion of the AL soliton[28, 32, 36]. So, the dynamics of a moving self-localized pulse, like the AL soliton in the framework of the IN-DNLS or the MSE will be subjected to two important effects. First one is the PN pinning arising from the lattice discreteness and second one is a nonlinear interaction potential, trying to trap or detrap the localized pulse. The cumulative effect of these two interactions is expected to be the collapse of the moving self-localized states to stable, but pinned solitons. This has indeed been observed in a numerical simulation[32]. From this discussion so far, it can be concluded that the sufficient condition to see the effect of discreteness on the dynamics of nonlinear excitations is that the discrete nonlinear equations must be nonintegrable. This nonintegrability can arise directly from the discretization of the continuous nonlinear equations or by adding integrability breaking terms to integrable discrete nonlinear equations.

Two important linear PDEs, which play very important roles in physics in linear systems are free-particle Schrödinger equation and the wave equation respectively[37]. These equations are, of course used to describe dynamics in continuous systems. The eigenvalue spectra of these equations are continuous function of a parameter, \mathbf{k} , called wave vector, with the $\overline{\lim} = \infty$ and the $\underline{\lim} = 0$. In case of systems, described by Schrödinger equation with a single-particle potential, an attractive potential will create localized states below the spectra and these are called 'bound states' of the

system[37]. Furthermore, in one $(1 + 1)$ dimensional systems, even an infinitesimally small attractive potential will create an exponentially localized bound state. On the other hand, wave equation being second order in time, even in $(1+1)$ dimension no attractive potential, however large can create bound states. On the contrary, one can get resonances from attractive potentials.

When the continuity in spatial variables is replaced by lattice continuity, the continuous spectra of linear PDEs fragments into bands. The number of bands will depend on the number of lattice points in the unit cell. When linear substitutional impurities are added to systems, described by a discrete Schrödinger equation, spatially localized states are formed in the gap between bands[37, 38]. We note that for a state to be localized and stable, it must be in the gap of the spectra. Furthermore, these states being exact eigenstates of the relevant Hamiltonian, are stationary localized states (SLS). For finite number linear impurities in $(1+1)$ dimension, it can be shown that the number of spatially exponentially localized states cannot exceed the number of impurities and there must be at least one exponentially localized state[37]. On the other hand, almost all states are exponentially localized in fully disordered $(1 + 1)$ dimensional systems[38]. However, with correlated disorder, it is possible to have some delocalized states[39, 40]. In stead of linear impurities, if finite number of nonlinear impurities are present, we again obtain SLS in such systems. This can be analytically shown in the systems, described by the DNLS[41, 42].

The spatially discrete analog of the continuous wave equation is the coupled mass-spring systems, with springs obeying the Hooke's law[37, 38]. Here again we get bands of eigenmodes, depending on the number of mass-spring units in a unit cell. The lowest band is called acoustic branch, which describes the collective motion of the masses. Other bands give optical phonons[43]. In systems containing finite number of mass impurities, only light mass impurities will form exponentially localized states above the acoustic band in $(1 + 1)$ dimension. Similar result is also obtained with impurity in springs[37]. Here also almost all states are exponentially localized in totally disordered systems, whether the disorder is in the mass or in the spring or in both[38]. However, no states are obtained below the acoustic branch. Most importantly, states around zero frequency remain delocalized[38]. In this system also, one can have nonlinear impurities, either in the spring, or in the on-site potential or in both. Any such impurity will produce SLS in the system[44]. We end this discussion by noting that both continuous and discrete linear systems cannot sustain any localized mode without broken continuous and lattice translational invariance respectively.

A uniform discrete nonlinear system will have lattice translational invariance. Similar to continuous nonlinear systems with translational invariance, nonlinearity in discrete systems can also generate localized modes by balancing the delocalization effect without requiring broken

periodicity. Such localized self-organization are the ILMs of discrete nonlinear systems. It is important to note that ILMs of a discrete nonlinear system are the exact eigenmodes of the nonlinear Hamiltonian, describing the system. As in continuous systems, ILMs in discrete systems can also be divided in two broad categories, solitons and breathers[11, 12, 13, 14, 15, 16, 17, 18, 19, 20, 21, 22]. In this case also the separation line is not always distinct. Consider for example the AL equation. The stationary one-soliton solutions of this equation are nothing but breathers[24, 25]. ILMs are predominantly occurring nonlinear excitations in discrete nonlinear systems. To understand this, we note that stable localized modes must always be either below the band or in band gaps[37]. So, the discreteness in spatial variables can provide a favorable mechanism for the formation and the stabilization of ILMs in discrete nonlinear systems by introducing finite bandwidths, and consequently accessible band edges. This, in turn increases the probability that the energy of a localized self-organization in a discrete nonlinear system will lie in the band gap. Again, the band width of a perfect linear discrete system depends on the magnitude of the inter-site coupling term. In a single band model, if such coupling is weak, we have a narrow band. A discrete nonlinear system with narrow bands is called anti-integrable. Such anti-integrable nonlinear systems are then expected to sustain nonlinearity induced localized modes in the band gaps by the above argument. There is indeed a mathematical proof of this in the literature[13, 14]. Of course, it is not necessary to have anti-integrable systems to have breathers. The existence of a breather solution in the N-AL equation has been shown[26]. In fact, in contrast to continuous nonlinear systems, in any general discrete nonlinear systems, particularly in nonintegrable systems, stationary breathers are predominantly occurring ILMs.

When localized states are formed below the lower band edge of a band, they are unstaggered or symmetric localized states. These states are symmetric under reflection through the center, and of course low energy localized modes of the system[26, 32]. Furthermore, these symmetric localized states can have its peak at a lattice site or in between two lattice sites. The first one is called on-site peaked unstaggered localized modes. The other one is called inter-site peaked unstaggered localized modes. When localized states are formed above the upper band edge of a band, they are staggered or antisymmetric localized states[32]. These states are antisymmetric under reflection and high energy excitations of a system. In case of staggered localized states, we analogously have odd-parity Sievers-Takeno mode (ST) as well as even-parity Page(P) mode[45, 46, 47]. It is also to be noted that staggered localized states have no analog in continuous systems[32]. Another kind of ILMs, called twisted localized modes can be found in nonlinear lattices[48, 49]. In this category also, we can have unstaggered as well as staggered localized modes[48, 49]. When these modes are stationary modes of the system, they are called sta-

tionary localized states (SLS). We emphasize again that SLS of any type, if they are true eigenmodes of nonlinear systems are also discrete breathers[11, 12]. They may be called trivial breathers.

Though it is possible to have in circumstances stationary ILMs in discrete integrable nonlinear systems, stationary ILMs are formed mostly in nonintegrable nonlinear systems. We discuss here the stationary ILMs of SLS type. We know that stationary solitons of AL equations are examples of SLS in integrable nonlinear equations, and these are also breather solutions of the same equation. We should, however not fail to note that though these breather solutions are band edge states, their widths are undetermined. On the other hand, the formation of SLS in discrete nonlinear systems depends critically on two factors, the inter-site hopping term which determines the width of bands in the corresponding linear systems and the strength of the nonlinearity, which determines the energy of the self organized localized formation. If the first term is predominant, the nonlinearity can produce at best localized modes near band edges. When localized states are formed near band edges, they are weakly localized. In other words, they have large widths and small amplitudes. Since, the movement of these localized modes does not require large scale rearrangement in the lattice, such localized modes can be made to move by applying small perturbing fields. As the movement of any unstaggered localized state will not require an inversion of orientation in any of sites, these states can easily move compared to its staggered counterpart under small perturbation. Again, in case of unstaggered localized states, inter-site peaked states will have larger widths and smaller amplitudes compared to its on-site peaked counterparts. So, inter-site peaked states can be made mobile easily by a small perturbation. In the other extreme where nonlinearity is strong, strong localized modes having nonzero amplitudes only at a few sites are formed. These are, of course high energy ILMs. Odd parity Sievers-Takeno (ST) modes and even parity P modes in strongly anharmonic lattices are examples of such strongly localized modes. Since these modes are formed from the acoustic branch of anharmonic lattices, they appear above the band and hence are staggered localized states. It is further found that ST modes are unstable to an infinitesimal perturbation. However, this mode is not destroyed by the perturbation. Instead, any perturbation makes it move[49]. On the other hand, P mode is stable and does not move by small perturbations. The mobility difference of these modes can be understood by the PN potential. Because of the distribution of amplitudes, ST modes are formed at the the maximum of the PN potential and the P modes at the bottom of this potential[50]. For the P mode to move then we need enough energy to excite this mode above the PN potential. Consequently, under a perturbation, not sufficient to take it out of the well, this mode will remain immobile. On the other hand, ST modes being at the maximum of the PN potential, no energy is needed to take it out of

the well. So, an infinitesimal perturbation can make it mobile. The mobility difference of on-site and inter-site peaked unstaggered localized modes to an infinitesimal perturbation can be understood by the same argument.

With this background, I plan to study here the formation of both unstaggered and staggered stationary localized states in systems described by IN-DNLS[32]. To this end, I plan to examine the dependence of the amplitude and width of the localized modes and also the eigenfrequency of these modes on the nonintegrability parameter of the equation. The energy of the localized modes are calculated from the Hamiltonian. To the best of my knowledge, a rudimentary asymptotic analysis of this problem is done using the lattice Green function approach[32, 51]. For the detailed study, I plan to use the discrete variational approach[23, 42, 52]. In nonlinear dynamics, the standard variational approach has been applied to continuous nonlinear equations to study problems of nonlinear pulse propagation in optical fibers, and to soliton dynamics in massive Thirring model, to mention a few[23, 53, 54, 55]. In the discrete variational approach, one directly proceeds to search for discrete solutions of the coupled discrete nonlinear evolution equations in a restricted subspace by imposing a suitable ansatz for the solution[23]. A procedure of averaging over the discrete dimensions leads to either a set of coupled ODE's or a set of coupled algebraic equations or both for the solution parameters. Therefore, this approach permits one to reduce the dimension of the problem from a set of many coupled equations to generally a much smaller set of equations, determined by the number of parameters in the ansatz to be determined. Clearly, this method is advantageous when the number of nonlinear equations is very large. This method has been applied to DNLS, for example to study problems of beam steering in nonlinear waveguide arrays[23], and also to understand the formation and stability of static and dynamical solitons in one dimensional systems and Cayley trees[42, 52]. We note in this context that equations like DNLS describe the evolution of canonical coordinates of the canonical phase space[23, 56]. On the other hand, AL, N -AL and IN-DNLS in their generic form describe the evolution of noncanonical coordinates in noncanonical phase spaces[24, 25, 26, 32, 56]. Since, these equations are derivable from Hamiltonians, the geometry of the dynamics is automatically symplectic[56]. The noncanonical symplectic structure of the dynamics is manifested in the structure of the Poisson brackets[8, 18, 26, 32, 36]. It is, however, to be noted that there exists a global nonsingular coordinate transformation for these equations, which transforms the noncanonical coordinates to canonical coordinates[36]. Therefore, these equations can also be described by canonical coordinates with canonical Lagrangian and Poisson brackets, having canonical symplectic structure[36, 56]. I shall, however proceed with the variational procedure with noncanonical

coordinates. I note that in Hamiltonian dynamics, the structure of the Poisson bracket is incorporated in the Lagrangian[36, 57]. But, my analysis is done with the appropriate functional, which is also obtainable from the Lagrangian. So, the noncanonical symplectic structure of the Poisson bracket does not pose any problem of finding SLS in IN-DNLS. The other side of this analysis is the following. It shows how the effective Lagrangian can be derived from the knowledge of the Hamiltonian and constants of motion using the analogous variational approach of finding eigenvalues in standard Sturm-Liouville problems[58]. In other words, I shall also show that it is possible to set up the variational problem for the determination of eigenvalues without the prior knowledge of the Lagrangian. Finally, I note that it has been seen in continuous nonlinear equations that when the variational method is applied to analyze solitary wave dynamics, the solitary wave solutions may show instability in some range of variational parameters. On the other hand, the correct dynamics may not show at all such instability. So, the variational method can produce false instabilities[52, 53]. This consideration also applies to discrete nonlinear evolution equations. However, I do not encounter any undesired instability in my solutions, which can be ascribed to the variational method. So, this aspect, even though important is not dealt with here.

The organization of the paper is as follows. In the formulation section below we present the basic equations to be studied. In the next section we present a set of results, coming from one particular formulation. In this section we also show that our formulation gives exact stationary localized states of the AL equation. In the next section we present another alternative formulation of the same problem. We then present the corresponding results. Finally, we summarize our main results in the summary section. Besides, this paper contains three important as well as relevant Appendices.

II. FORMALISM

A. General derivation of the nonlinear IN-DNLS equation and the variational formulation of the corresponding eigenvalue problem

We consider a dynamical system having $2N$ generalized noncanonical coordinates, $\{\phi_n, \phi_n^*\}$, $n = 1, \dots, N$ in a symplectic manifold[56]. Let U and V be any two general dynamical variables of the system. Any symplectic manifold has a natural Poisson bracket structure, defined in terms of the inverse of the symplectic structure function[56]. So, we now define the following noncanonical Poisson bracket to characterize the manifold[8, 32, 36].

$$\{U, V\}_{\{\phi, \phi^*\}} = i \sum_{n=1}^N \left(\frac{\partial U}{\partial \phi_n} \frac{\partial V}{\partial \phi_n^*} - \frac{\partial V}{\partial \phi_n} \frac{\partial U}{\partial \phi_n^*} \right) (1 + \mu |\phi_n|^2). \quad (2.1)$$

We now consider the following Hamiltonian, \tilde{H} .

$$\tilde{H} = - \sum_n (\phi_n^* \phi_{n+1} + \phi_{n+1}^* \phi_n) - 2\nu \sum_n |\phi_n|^2 + 2\nu \sum_n \ln[1 + |\phi_n|^2]; \quad (2.2)$$

which is obtained from the original IN-DNLS Hamiltonian, H through the transformations, $\phi_n \rightarrow \sqrt{\mu} \phi_n$, $n \in Z$ and $\nu \rightarrow \frac{\nu}{\mu}$ [32, 36]. The corresponding Lagrangian $\tilde{\mathcal{L}}$ in the scaled variables[36, 57] is

$$\tilde{\mathcal{L}} = \frac{i}{2} \sum_n (\dot{\phi}_n \phi_n^* - \dot{\phi}_n^* \phi_n) \frac{\ln[1 + |\phi_n|^2]}{|\phi_n|^2} - \tilde{H}. \quad (2.3)$$

The dynamical evolution of the n -th generalized coordinate, ϕ_n , can then be obtained by using Eq.(2.1) and Eq.(2.2).

$$\begin{aligned} i \dot{\phi}_n &= (1 + |\phi_n|^2) \frac{\partial \tilde{H}}{\partial \phi_n^*} \\ &= -(1 + |\phi_n|^2)(\phi_{n+1} + \phi_{n-1}) \\ &\quad - 2\nu |\phi_n|^2 \phi_n, \end{aligned} \quad (2.4)$$

for $n \in Z$ [32, 36]. The other set of equations is obtained by conjugation. The same equation can be obtained from the Lagrangian by using the standard Lagrangian equations of motion. We note that under the global gauge transformation, $\phi_n \rightarrow \phi_n e^{i\alpha}$, Eqs.(2.2), (2.3) and (2.4) remain invariant. It can also be shown from Eq.(2.4) that $\tilde{\mathcal{N}} = \sum_n \ln[1 + |\phi_n|^2]$ is a constant of motion[32]. We now assume that $\phi_n = \lambda^n \Psi_n \exp(-i\omega t)$, $n \in Z$ where $\lambda = \pm 1$. Furthermore, Ψ_n , $n \in Z$ are taken real[32]. Then from Eq.(2.4), we get

$$\begin{aligned} (\hat{\Omega} \hat{\Psi})_n &= \omega \Psi_n + \lambda (1 + \Psi_n^2) (\Psi_{n+1} + \Psi_{n-1}) \\ &\quad + 2\nu \Psi_n^3 = 0. \end{aligned} \quad (2.5)$$

This is a nonlinear eigenvalue problem and its solutions give frequencies of stationary localized states of IN-DNLS equation[32]. Introducing the above ansatz for ϕ_n , $n \in Z$ in $\tilde{\mathcal{N}}$, and \tilde{H} , we get

$$\tilde{\mathcal{N}} = \sum_n \ln[1 + \Psi_n^2], \quad (2.6)$$

$$\begin{aligned} \tilde{H} &= -2\lambda \sum_n \Psi_n \Psi_{n+1} - 2\nu \sum_n \Psi_n^2 + 2\nu \tilde{\mathcal{N}} \\ &= \tilde{H}_0 + 2\nu \tilde{\mathcal{N}}. \end{aligned} \quad (2.7)$$

We define next

$$\tilde{F} = \tilde{H} - \Lambda \tilde{\mathcal{N}} \quad (2.8)$$

where Λ is the Lagrange multiplier[59]. Setting $\delta \tilde{F} = 0$, we get back Eq.(2.5), when $\Lambda = \omega$. It is also important to note that the functional, \tilde{F} can also be obtained from $\tilde{\mathcal{L}}$ after introducing the ansatz. In Appendix A, I plan to discuss the importance of the functional, \tilde{F} .

B. Variational approach with sech ansatz

We first note that the system described by IN-DNLS equation, Eq.(2.4) has lattice translational invariance. So, this system can only form ILMs, arising from the competition between the localizing nonlinearity and the dispersion from the inter-site hopping[9]. As the corresponding linear system is a discrete single band system, this further enhances the propensity of formation of ILMs either below or above the band. According to the theory of localization, any self-localized state in 1-d systems will have exponential localization in the following sense. The amplitude, Ψ_n of the localized mode at the n -th site will show exponential decay with $|n|$ for large values of $|n|$ [37, 38]. We should also keep in mind that a modulus function($|\dots|$) cannot appear in physical problem in its generic form. This type of functions can only be obtained in any physical problem in the asymptotic limit. Furthermore, when $\nu = 0$, Eq.(2.4) becomes the well known AL equation[24, 25, 32]. The one-soliton solution of Ablowitz-Ladik(AL) equation can either be static or dynamic. For both cases, it has the sech profile, which satisfies also the other requirement for localized states in one dimension. So, we use the ansatz, $\Psi_n = \Phi \frac{1}{\cosh \beta(n - x_0)}$, $n \in Z$. This ansatz has also been used in the previous analysis[32]. For on-site peaked and ST like localized states, $x_0 = 0$, and for inter-site peaked and P like states, $x_0 = \pm \frac{1}{2}$ [23, 45, 46, 47]. We further write $\Phi^2 = \Psi$. While β^{-1} gives the half-width of localization, Φ denotes the maximum amplitude of the states. Now, introduction of this ansatz in the functional \tilde{F} makes it an algebraic function of the parameters of the ansatz,

$$\tilde{\mathcal{F}}(\Psi, \beta, \lambda, x_0) = \tilde{H}(\Psi, \beta, \lambda, x_0) - \Lambda \tilde{\mathcal{N}}(\Psi, \beta, x_0), \quad (2.9)$$

and we need to find relative extrema of \tilde{F} with respect to variables, Ψ and β [59]. The finding of relative extrema with respect to these two variables, Ψ and β means that

$d\tilde{F} = 0$ should imply the following equations[59].

$$\frac{\partial \tilde{H}_0}{\partial \Psi} - \Lambda_1 \frac{\partial \tilde{N}}{\partial \Psi} = 0 \quad (2.10)$$

$$\frac{\partial \tilde{H}_0}{\partial \beta} - \Lambda_1 \frac{\partial \tilde{N}}{\partial \beta} = 0, \quad (2.11)$$

where $\Lambda_1 = \Lambda - 2\nu$. For what follows next, we assume that $\frac{\partial \tilde{N}}{\partial \Psi} \neq 0$. Then from Eqs.(2.10) and (2.11), we find that

$$\Lambda = \omega = 2\nu + \frac{\frac{\partial \tilde{H}_0}{\partial \Psi}}{\frac{\partial \tilde{N}}{\partial \Psi}} \quad (2.12)$$

and also

$$f(\Psi, \beta, \lambda, x_0) = \{\tilde{H}_0, \tilde{N}\}_{\{\beta, \Psi\}} = 0. \quad (2.13)$$

The other required equation is

$$\tilde{N}(\Psi, \beta, x_0) = C = \text{Constant}. \quad (2.14)$$

We note that we have three unknowns, namely Λ, Ψ and β . But, we also have three independent equations to solve for these unknowns. Hence, the problem is well-posed.

C. Calculation of \tilde{H}_0 and \tilde{N}

Introducing the expression of Ψ_n , $n \in Z$ in \tilde{H}_0 and \tilde{N} we get

$$\tilde{H}_0(\Psi, \beta, \lambda, x_0) = -2\lambda\Psi S_1(\beta, x_0) - 2\nu\Psi S_2(\beta, x_0), \quad (2.15)$$

where

$$S_1(\beta, x_0) = \sum_{n=-\infty}^{\infty} \frac{1}{\cosh \beta(n-x_0) \cosh \beta(n+1-x_0)}$$

$$S_2(\beta, x_0) = \sum_{n=-\infty}^{\infty} \frac{1}{\cosh^2 \beta(n-x_0)}$$

$$\tilde{N}(\Psi, \beta, x_0) = \sum_{n=-\infty}^{\infty} Y_n(\Psi, \beta, x_0) \quad (2.16)$$

where

$$Y_n(\Psi, \beta, x_0) = \ln \left[1 + \frac{\Psi}{\cosh^2 \beta(n-x_0)} \right].$$

To evaluate $S_1(\beta, x_0)$, $S_2(\beta, x_0)$ and $\tilde{N}(\Psi, \beta, x_0)$, we make use of the famous Poisson's sum formula[23, 26,

28, 31, 43] which reads

$$\sum_{n=-\infty}^{\infty} f(n\beta) = \frac{1}{\beta} \int_{-\infty}^{\infty} dy [1 + 2 \sum_{s=1}^{\infty} \cos(\frac{2\pi s y}{\beta})] f(y). \quad (2.17)$$

This application yields

$$S_1(\beta, x_0) = \frac{2}{\sinh \beta}, \quad (2.18)$$

$$S_2(\beta, x_0) = \frac{2}{\beta} + \frac{4}{\beta} \sum_{s=1}^{\infty} \Gamma_s(\beta, x_0), \quad (2.19)$$

where

$$\Gamma_s(\beta, x_0) = \cos 2\pi s x_0 \frac{\frac{\pi^2 s}{\beta}}{\sinh \frac{\pi^2 s}{\beta}}.$$

$$\begin{aligned} \sqrt{\Psi(1+\Psi)} \frac{\partial \tilde{N}}{\partial \Psi} &= \frac{2}{\beta} \operatorname{arcsinh} \sqrt{\Psi} \\ &+ \frac{2\pi}{\beta} \sum_{s=1}^{\infty} \cos 2\pi s x_0 T_s(\Psi, \beta), \end{aligned} \quad (2.20)$$

where

$$T_s(\Psi, \beta) = \frac{\sin [\frac{2\pi s}{\beta} \operatorname{arcsinh} \sqrt{\Psi}]}{\sinh \frac{\pi^2 s}{\beta}}.$$

We now define a function, $f_1(\beta, \nu, \lambda, x_0)$

$$f_1(\beta, \nu, \lambda, x_0) = \frac{\sinh \beta}{1 + \lambda \nu \frac{\sinh \beta}{\beta} S_3(\beta, \nu, \lambda, x_0)}, \quad (2.21)$$

where

$$S_3(\beta, \nu, \lambda, x_0) = 1 + 2 \sum_{s=1}^{\infty} \cos 2\pi s x_0 \frac{\frac{\pi^2 s}{\beta}}{\sinh \frac{\pi^2 s}{\beta}}.$$

Now, with this definition, we have

$$\tilde{H}_0 = -4\lambda \frac{\Psi}{f_1(\beta, \nu, \lambda, x_0)} \quad (2.22)$$

$$\frac{\partial \tilde{H}_0}{\partial \Psi} = - \frac{4\lambda}{f_1(\beta, \nu, \lambda, x_0)} \quad (2.23)$$

$$\frac{\partial \tilde{H}_0}{\partial \beta} = -4\lambda \Psi \frac{\partial \frac{1}{f_1(\beta, \nu, \lambda, x_0)}}{\partial \beta}. \quad (2.24)$$

Again from Eq.(2.20), we have

$$\tilde{\mathcal{N}}(\Psi, \beta, x_0) = \frac{2}{\beta} (\text{arc sinh } \sqrt{\Psi})^2 + 4 \sum_{s=1}^{\infty} \cos 2\pi s x_0 \frac{\sin^2 \left(\frac{\pi s}{\beta} \text{arc sinh } \sqrt{\Psi} \right)}{s \sinh \frac{\pi^2 s}{\beta}}, \quad (2.25)$$

and from Eq.(2.25) we in turn get

$$\begin{aligned} \frac{\partial \tilde{\mathcal{N}}}{\partial \beta} &= -\frac{2}{\beta^2} (\text{arc sinh } \sqrt{\Psi})^2 \\ &- \frac{4 \pi \text{arc sinh } \sqrt{\Psi}}{\beta^2} \sum_{s=1}^{\infty} \cos 2\pi s x_0 \frac{\sin \left(\frac{2 \pi s}{\beta} \text{arc sinh } \sqrt{\Psi} \right)}{\sinh \frac{\pi^2 s}{\beta}} \\ &+ \frac{4 \pi^2}{\beta^2} \sum_{s=1}^{\infty} \cos 2\pi s x_0 \frac{\sin^2 \left(\frac{\pi s}{\beta} \text{arc sinh } \sqrt{\Psi} \right)}{\sinh \frac{\pi^2 s}{\beta}} \coth \frac{\pi^2 s}{\beta}. \end{aligned} \quad (2.26)$$

The calculation of Eq.(2.25) is given in Appendix B.

In our variational formulation, in principle x_0 is another parameter to be determined from the extrema of the functional, \tilde{F} (Eq.(2.8)). Now, the extremization of \tilde{F} with x_0 inclusive will yield along with Eqs.(2.10) and (2.11), the following equation.

$$\frac{\partial \tilde{H}_0}{\partial x_0} - \Lambda_1 \frac{\partial \tilde{\mathcal{N}}}{\partial x_0} = 0. \quad (2.27)$$

But, from Eqs.(2.21), (2.22) and (2.25), it can be easily proved that as $0 \leq |x_0| < 1$, $x_0 = 0, \pm \frac{1}{2}$.

III. THE VARIATIONAL FORMULATION WITH $\tilde{\mathcal{N}}$ CONSTANT : RESULTS AND DISCUSSION

A. Ablowitz-Ladik limit

In the Ablowitz-Ladik limit, $\nu = 0$. To probe this limit, we evaluate relevant functions and their derivatives along the curve $\Psi = \sinh^2 \beta$. Along this curve, from Eqs.(2.20), (2.25) and (2.26) we have

$$\tilde{\mathcal{N}}(\Psi, \beta, x_0) = 2 \beta \quad (3.1)$$

$$\frac{\partial \tilde{\mathcal{N}}}{\partial \beta} = -2 \quad (3.2)$$

$$\frac{\partial \tilde{\mathcal{N}}}{\partial \Psi} = \frac{2}{\sinh \beta \cosh \beta}. \quad (3.3)$$

Since, $\nu = 0$ in this case, we also have from Eqs.(2.21) to (2.24)

$$\frac{\partial \tilde{H}_0}{\partial \Psi} = -\frac{4 \lambda}{\sinh \beta} \quad (3.4)$$

$$\frac{\partial \tilde{H}_0}{\partial \beta} = 4 \lambda \cosh \beta. \quad (3.5)$$

We find from Eqs.(3.2) to (3.5) that $f(\Psi, \beta, \lambda, x_0) = \{\tilde{H}_0, \tilde{\mathcal{N}}\}_{\{\beta, \Psi\}} = 0$. Furthermore, from Eqs.(2.12), (3.3) and (3.4) we get $\omega = -2 \lambda \cosh \beta$. The energy, $\tilde{E} = \tilde{H} = -4 \lambda \sinh \beta$. Due to positive semi-definiteness of $\tilde{\mathcal{N}}$, we get from Eq.(3.1) that β should also be positive semidefinite. This is consistent with the one-soliton solution of Ablowitz-Ladik equation.

We now consider the case of $\nu \neq 0$. For convenience, we define

$$g(\beta, x_0) = \frac{1}{\beta} \left[1 + 2 \sum_{s=1}^{\infty} \cos 2\pi s x_0 \frac{\frac{\pi^2 s}{\beta}}{\sinh \frac{\pi^2 s}{\beta}} \right] \quad (3.6)$$

Along the line $\Psi = \sinh^2 \beta$, we find that

$$\begin{aligned} f(\Psi, \beta, \lambda, x_0) &= \{\tilde{H}_0, \tilde{\mathcal{N}}\}_{\{\beta, \Psi\}} \\ &= -8 \nu g(\beta, x_0) \tanh \beta \frac{d \ln A_0(\beta, x_0)}{d \beta} \end{aligned} \quad (3.7)$$

where $A_0(\beta, x_0) = \sinh \beta g(\beta, x_0)$. When $\beta \rightarrow 0$, $\tanh \beta \frac{d \ln A_0(\beta, x_0)}{d \beta} \rightarrow \frac{\beta^2}{3}$, and consequently $f(\Psi, \beta, \lambda, x_0) \sim -\frac{8\nu}{3} \beta^2$, provided ν is finite. So, when $(\nu \beta^2) \sim o(1)$, $\Psi = \sinh^2 \beta$ is an asymptotic solution of a localized state with a large width and a small amplitude. Eigenvalue, ω and energy, $\tilde{E} = \tilde{H}$ of these localized states are

$$\begin{aligned} \omega &= 2 \nu - 2(\lambda + \nu A_0) \cosh \beta \\ &\sim -2 \lambda - \left(\lambda + \frac{4\nu}{3} \right) \beta^2, \end{aligned} \quad (3.8)$$

and

$$\begin{aligned} \tilde{E} &= -4 \lambda \beta - 4 \nu \beta \left[\frac{A_0 \sinh \beta}{\beta} - 1 \right] \\ &\sim -4 \lambda \beta - \frac{4 \nu}{3} \beta^3. \end{aligned} \quad (3.9)$$

So, according to this asymptotic analysis, when $\nu \neq 0$, the nonintegrability parameter, ν and the width parameter β of the SLS are not independent of each other.

B. Stationary localized states from IN-DNLS

We now consider various mathematical aspects of the formation of stationary localized states in IN-DNLS. We consider first Eq.(2.14) along with Eq.(2.25). We restrict ourselves to $\beta \geq 0$, which is necessary to keep Ψ positive semi-definite. Furthermore, in the following analysis, we assume that $\beta \leq 1$. In this situation, we can ignore infinite sums in Eq.(2.21) and in Eq.(2.25). Due to this approximation, Eq.(2.25) yields $\Psi = \sinh^2 \alpha \sqrt{\beta}$ where α is a constant, as required by Eq.(2.14). Since, the right hand side of Eq.(2.14) is taken to be a number constant, $C = 2.0 \alpha^2$, we have $\frac{d\tilde{N}}{d\beta} = 0$ irrespective of the value of β . This, in turn gives

$$\frac{d\Psi}{d\beta} = - \frac{\frac{\partial \tilde{N}}{\partial \beta}}{\frac{\partial \tilde{N}}{\partial \Psi}}. \quad (3.10)$$

Now introducing Eq.(3.10) in Eq.(2.13), we get $\frac{d\tilde{H}_0}{d\beta} = 0$. In other words, permissible values of β are determined from the extrema of \tilde{H}_0 as a function of β . From the functional dependence of \tilde{H}_0 , and Ψ on β , we ultimately get

$$\begin{aligned} g_1(\alpha, \beta) &= \frac{\beta}{\sinh \beta} \cosh \beta \frac{\tanh \alpha \sqrt{\beta}}{\alpha \sqrt{\beta}} - 1 \\ g_2(\alpha, \beta) &= 1 - \frac{\tanh \alpha \sqrt{\beta}}{\alpha \sqrt{\beta}} \\ \nu \lambda &= \frac{\beta}{\sinh \beta} \frac{g_1(\alpha, \beta)}{g_2(\alpha, \beta)}. \end{aligned} \quad (3.11)$$

We note that for a given value of the parameter, α , β is determined by the nonintegrability parameter, ν . Furthermore, Eq.(3.11) yields two positive values of β as roots, if two conditions, namely $\nu \lambda \geq 0$ and $|\nu| < |\nu_{critical}|$. The behavior of the smaller root (β_s) as a function of ν for $\lambda = 1$ and $\alpha = 0.5$ and 0.25 are shown in Fig.1. In Fig.2 we present the variation of β_s as a function of the parameter, α for various values of $\nu \geq 0$. It should be noted from these figures that $\beta_s \leq 1$ for these values of α and the chosen interval of ν . So, the neglect of infinite sums in Eqs.(2.21) and (2.25) is justified. It is a simple exercise to see from Eq.(3.11) that when $|\nu| \rightarrow 0$, $\beta_s \rightarrow \alpha^2$. Then, for small values of ν the asymptotic solution is the AL stationary localized state solution. This is a very important result. This asymptotic analysis reveals that this stationary localized state solution of IN-DNLS continuously moves to the AL stationary localized state solution when $\nu \rightarrow 0$ from either side. It is further important to note from Fig.2 that for $\alpha \ll 1$, we have $\alpha \approx \sqrt{\frac{\beta_s}{1.0 + \nu \lambda}}$, $\nu \lambda \geq 0$. Consequently, $\sqrt{\Psi} \approx \sinh \frac{\beta_s}{\sqrt{1.0 + \nu \lambda}}$. But, as for this range of argument, $\sinh x \approx x$, we have $\sqrt{\Psi} \sim \frac{\beta_s}{\sqrt{1.0 + \nu \lambda}}$. This agrees with the existing asymptotic analysis[32].

The variation of the large root, β_l as a function of $\nu \lambda$ for various values of α is shown in Fig.3. Again, by

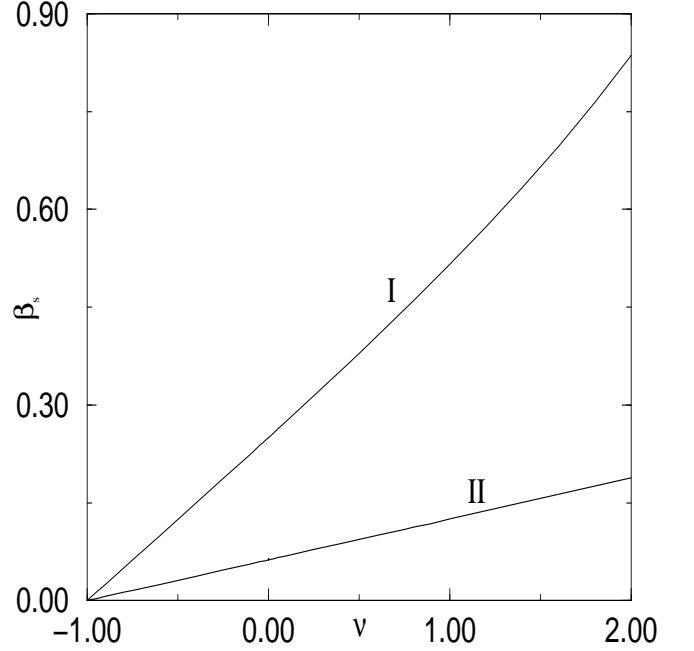


FIG. 1: This figure shows the variation of the smaller root, β_s of Eq.(3.11) as a function of the nonintegrability parameter, ν . Since $\lambda = 1$, these states are unstaggered stationary localized states. Curve I : $\alpha = 0.5$ and Curve II : $\alpha = 0.25$.

comparing Fig.1 and Fig.3, we see that as ν increases, the large root, β_l , of Eq.(3.11) decreases from ∞ , while the other root, β_s increases from zero. So, for a given α , the value of $\nu_{critical}$ is determined by the inflection point of \tilde{H}_0 . This then implies that equations to solve for $\beta_{critical}$, and $\nu_{critical}$ are obtained by setting both $\frac{d\tilde{H}_0}{d\beta} = 0$ and $\frac{d^2\tilde{H}_0}{d\beta^2} = 0$. While the first condition gives Eq.(3.11), the second condition yields Eq.(3.12) as shown below.

$$\begin{aligned} g_3(\beta) &= \frac{\tanh \sqrt{\beta}}{\sqrt{\beta}} \quad \text{and} \quad g_4(\beta) = \frac{\beta}{\sinh \beta}, \\ g_5(\alpha, \beta) &= 1 - g_3(4\alpha^2\beta) - 4 g_3(4\alpha^2\beta)(1 - g_3(\alpha^2\beta)), \\ g_6(\alpha, \beta) &= 1 - g_3(4\alpha^2\beta) (1 + 4 \cosh \beta g_4(\beta)), \\ g_7(\alpha, \beta) &= g_4(\beta) g_3^2(\alpha^2\beta) (\beta^2 + 2 g_4^2(\beta)), \\ g_8(\alpha, \beta) &= -2\nu \frac{\alpha^2}{\beta^2} \cosh 2\alpha\sqrt{\beta} g_5(\alpha, \beta), \\ g_9(\alpha, \beta) &= -2 \lambda \frac{\alpha^2}{\beta^2} \cosh 2\alpha \sqrt{\beta} g_4(\beta) g_6(\alpha, \beta), \\ g_{10}(\alpha, \beta) &= -4 \lambda \frac{\alpha^2}{\beta^2} \cosh^2 \alpha \sqrt{\beta} g_7(\alpha, \beta), \\ g_8(\alpha, \beta) + g_9(\alpha, \beta) + g_{10}(\alpha, \beta) &= 0. \end{aligned} \quad (3.12)$$

We again note that $\lambda = \pm 1$ and ν in Eq.(3.12) is given by Eq.(3.11). Of course, $\nu \lambda$ is positive. We find from

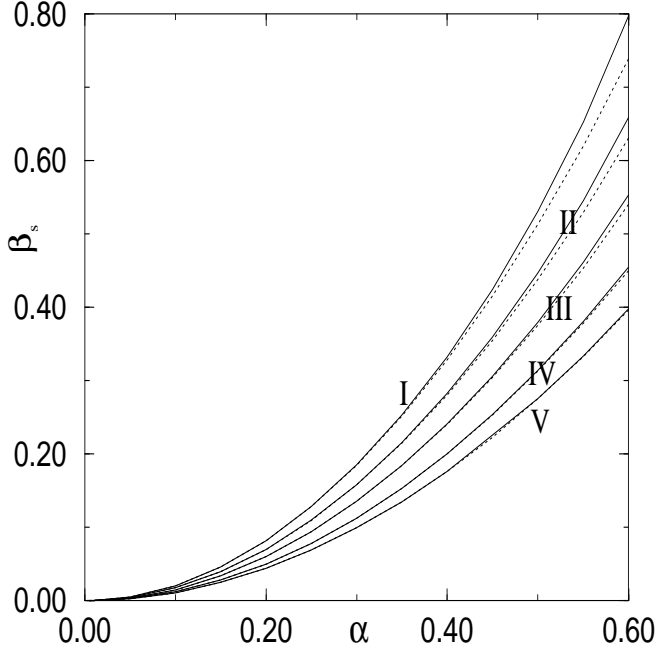


FIG. 2: This figure shows the variation of the smaller root, β_s of Eq.(3.11) as a function of the parameter, α for various values of the nonintegrability parameter, ν . Since $\lambda = 1$, these states are unstaggered stationary localized states. Curve I : $\nu = 1.05$, Curve II : $\nu = 0.75$, Curve III : $\nu = 0.5$, Curve IV : $\nu = 0.25$, and Curve V : $\nu = 0.10$. Each curve is associated with a dotted curve which shows the variation of $\alpha^2(1 + \nu\lambda)$ as a function of α for the corresponding value of ν .

Eq.(3.12) that when $\alpha \rightarrow 0$, $\nu_{\text{critical}} \rightarrow \infty$. Again, when $\alpha \gg 1$, $\nu_{\text{critical}} \sim 0$. The functional dependence of ν_{critical} on α is shown in Fig.4.

The other important case is where $\nu\lambda < 0$. This means that either we have an unstaggered state with $-\nu$ or a staggered state with $+\nu$. In this case if $|\nu\lambda| > 1$, both roots of Eq.(3.11) are negative. Inasmuch as $\tilde{\mathcal{N}}(\psi, \beta, x_0)$ is positive semi-definite, it is easy to see from Eq.(2.25) that this is not permissible. For this case, from Eq.(3.11) as expectedly we obtain that when $\nu\lambda \rightarrow -1+$, $\beta \rightarrow 0$, and when $\nu\lambda \rightarrow 0-$, $\beta \rightarrow \alpha^2$. See both Fig.1 and Fig.5. Inasmuch as for $\alpha \leq 1$, permissible values of $\beta_s \leq 1$, the neglect of infinite sums in Eqs.(2.21) and (2.25) is again well justified. The variation of β_s as a function of ν for $\alpha = 1.0, 0.75, 0.5, 0.25$, and 0.10 are shown in Fig.5. It is seen from Fig.6 that when $\nu\lambda < 0$, $\alpha = \sqrt{\frac{\beta_s}{1.0 + \nu\lambda}}$ is a very good approximation[32]. Another important aspect is in Fig.7, which shows that for a given $\nu > 0$, the staggered SLS ($\lambda = -1$) has larger width than the corresponding unstaggered SLS ($\lambda = 1$). So, the SLS for $\nu\lambda < 0$ are basically localized states with large widths and small amplitudes. As for eigenvalues of these stationary localized states, introducing Eqs.(2.20) and (2.23)

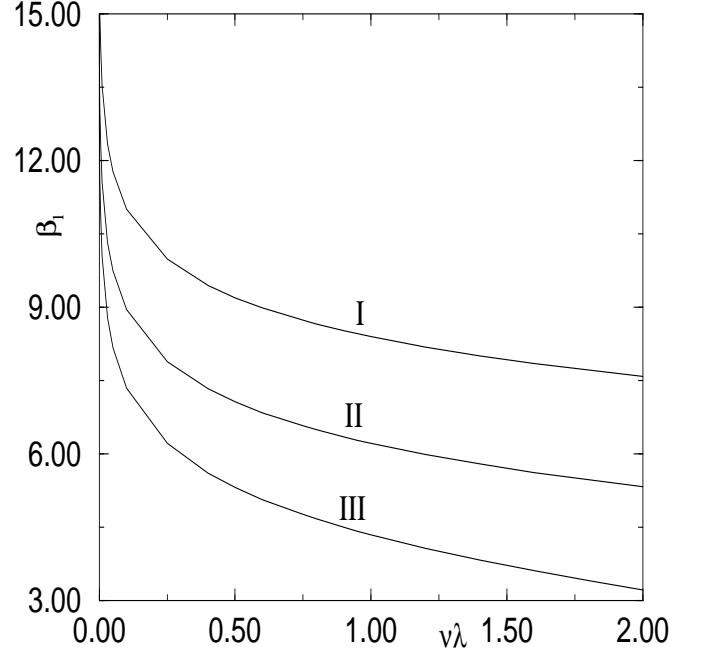


FIG. 3: This figure shows the variation of the larger root, β_l of Eq.(3.11) as a function of $\nu\lambda$. If $\lambda = 1$, these states are then unstaggered stationary localized states. Curve I : $\alpha = 0.1$ and Curve II : $\alpha = 0.25$, and Curve III : $\alpha = 0.50$.

into Eq.(2.12) and using the same approximation as used for finding the roots of Eq.(3.11), we obtain that

$$\begin{aligned} \omega &= -2\nu \left[\frac{\sinh 2\alpha\sqrt{\beta}}{2\alpha\sqrt{\beta}} - 1 \right] \\ &\quad - 2\lambda \frac{\beta}{\sinh \beta} \frac{\sinh 2\alpha\sqrt{\beta}}{2\alpha\sqrt{\beta}}. \end{aligned} \quad (3.13)$$

The energy of these stationary states is given by

$$\begin{aligned} \tilde{E} &= \tilde{H} = \tilde{H}_0 + 2\nu\tilde{\mathcal{N}} \\ &= -4\lambda \frac{\sinh^2 \alpha \sqrt{\beta}}{\sinh \beta} \\ &\quad - 4\nu\alpha^2 \left[\frac{\sinh^2 \alpha \sqrt{\beta}}{\alpha^2 \beta} - 1 \right]. \end{aligned} \quad (3.14)$$

β in Eqs.(3.13) and (3.14) is the root of Eq.(3.11). For $\beta = \beta_s$ and α not too large, these equations are well justified. We already noted that when $\nu = 0$, $\beta_s = \alpha^2$. Furthermore, $|\nu\lambda| \ll 1$ and also $\alpha \ll 1$, $\beta_s \rightarrow \alpha^2$. We obtain the respective limiting results for these cases from Eqs.(3.13) and (3.14).

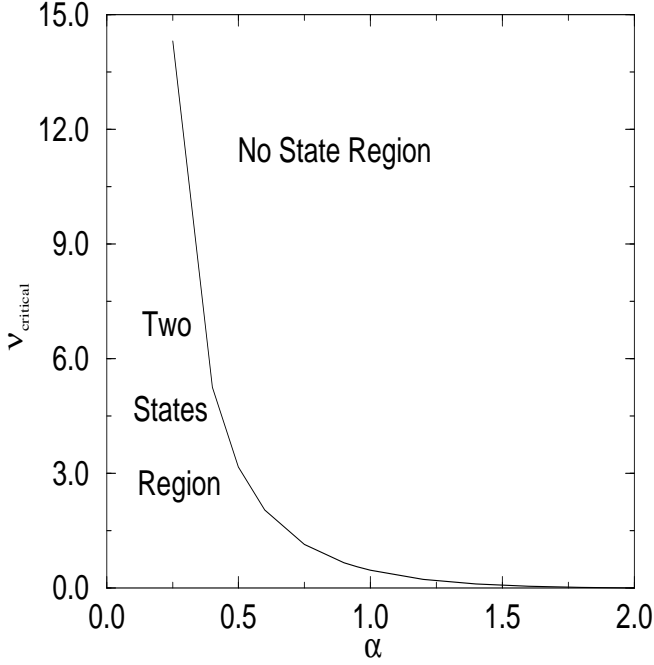


FIG. 4: This figure shows the variation of ν_{critical} as a function of the parameter, α for unstaggered stationary localized states, $\lambda = 1$. ν_{critical} is obtained from Eqs.(3.11) and (3.12) in the text. Note that the curve separates the two states region from the no state region.

C. Stability and position of stationary localized states of IN-DNLS

We now discuss the issue of stability of these stationary localized states. We note first that when $\nu = 0$, the resulting nonlinear equation is the AL equation, which has both unstaggered and staggered stationary localized states. These are basically band edge states. Our variational calculation correctly produces these states of the AL equation, by letting $\beta_s \rightarrow \alpha^2$ as $|\nu| \rightarrow 0$. See Fig.1 and Fig.5. Over and above it suggests another state for which $\beta_l = \infty$. This can be easily seen in Eq.(3.11). It is again seen from Fig.1 and Fig.2 that for any α , introduction of any ν , however small, with $\nu\lambda > 0$ makes $\beta_s > \alpha^2$. We observe that β_s^{-1} gives the half-width of the localized state. So, for these localized states, the half-width reduces with increasing ν . Since for $\lambda = 1$ and $\nu > 0$ ($\nu\lambda > 0$) implies that the on-site nonlinear trapping potential is attractive, any positive enhancement of ν should reduce the half-width of the SLS by effectively reducing the inter-site hopping. Whether a given ν defines an attractive or a repulsive potential also depends upon the value of λ . So, the above argument will hold good whenever $\nu\lambda > 0$. When $\nu\lambda$ is positive, unstaggered stationary localized states characterized by β_s are stable.

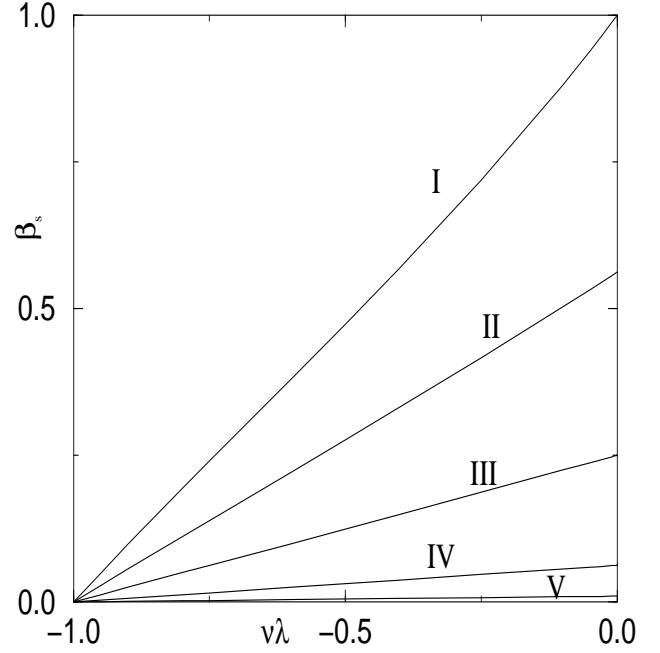


FIG. 5: This figure shows the variation of the smaller root, β_s of Eq.(3.11) as a function of $\nu\lambda$ for $\nu\lambda < 0$ for various values of the nonintegrability parameter, α . For $\lambda = -1$, these states are staggered stationary localized states. Curve I : $\alpha = 1.0$, Curve II : $\alpha = 0.75$, Curve III : $\alpha = 0.5$, Curve IV : $\alpha = 0.25$, and Curve V : $\alpha = 0.10$.

On the other hand, for $\nu = 0$, if there is any stationary localized state corresponding to $\beta_l = \infty$, it is a state with a peak of infinite height at a given site with a half-width of a few sites. Again, we see from Fig.3 that for any α , when $\nu\lambda$ increases, β_l decreases. This means that the half-width increases. On the other hand, the introduction of ν with $\nu\lambda > 0$ should reduce the half-width, as our argument suggests. Hence, stationary localized states corresponding to β_l are unstable. These states, if exist in this system, will be unstable towards perturbation.

Consider next the case where $\nu\lambda < 0$. In this case, we have either staggered localized states for positive ν , or unstaggered localized states for negative ν . First of all, there is only one set of stationary localized states. Furthermore, $0 \leq \beta_s \leq \alpha^2$ for $-1 \leq \nu\lambda \leq 0$. See Fig.5. Since, for $\nu > 0$, staggered localized states are stabilized by increasing the half-width (see Fig.7), states characterized by β_s are stable. For ν negative and $\lambda = 1$, or $\nu > 0$ and $\lambda = -1$, the on-site nonlinear potential is repulsive. So, the expansion of the half-width with decreasing ν is energetically favorable (see Fig.7).

So far our analysis did not include the effect of x_0 , the position of the peak on the formation of stationary localized states and their stability. But, this is also an important part of the problem. However, even a semi-rigorous investigation of this problem in this formulation requires

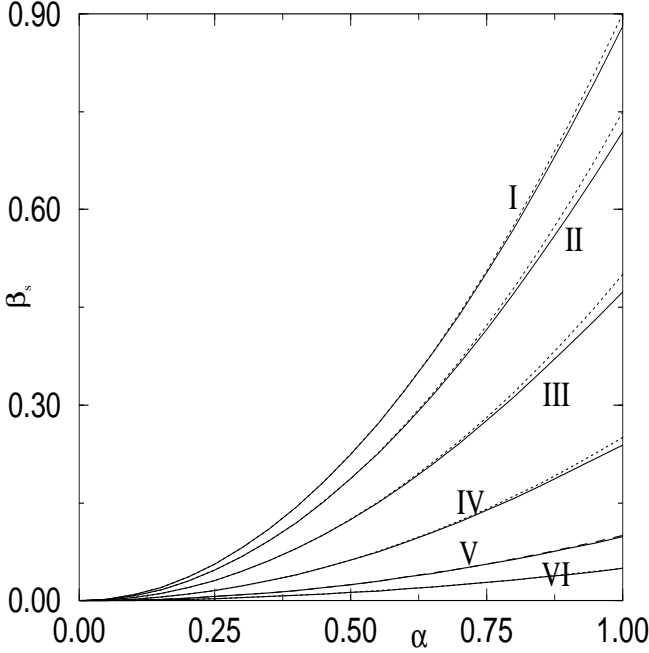


FIG. 6: This figure shows the variation of the smaller root, β_s of Eq.(3.11) as a function of the parameter, α for various values of the nonintegrability parameter, ν . Since $\lambda = -1$, these states are staggered stationary localized states. Curve I : $\nu = 0.1$, Curve II : $\nu = 0.25$, Curve III : $\nu = 0.5$, Curve IV : $\nu = 0.75$, Curve V : $\nu = 0.90$ and Curve VI : $\nu = 0.95$. Each curve is also associated as in Fig.2 with a dotted curve which shows the variation of $\alpha^2(1+\nu\lambda)$ as a function of α for the corresponding value of ν .

the analytical solution of Ψ as exactly as possible from Eq.(2.25). As there is no simple analytical way of solving Eq.(2.25) for Ψ , one can take recourse to approximation methods like, the method of *successive substitutions*[60]. I shall describe in Appendix C how this method can be used to get approximate dependence on x_0 , of β , ω and E of the SLS. Of course, the other possibility is to find real positive roots of Eq.(2.25) graphically. Inasmuch as the exact analytical solution of Ψ as a function of β is difficult in this approach, we shall not follow the present line of investigation further. On the contrary, we shall show next how the exact dependence of the parameter, β , the frequency ω and the energy E of the SLS on x_0 can be obtained by a rational alternation in the variational procedure.

IV. THE VARIATIONAL FORMULATION WITH \tilde{H}_0 CONSTANT : RESULTS AND DISCUSSION

Since, \tilde{H} and $\tilde{\mathcal{N}}$ (Eq.2.2) and Eq.(2.6) respectively) are two constants of motion, from the expression of \tilde{H} , we

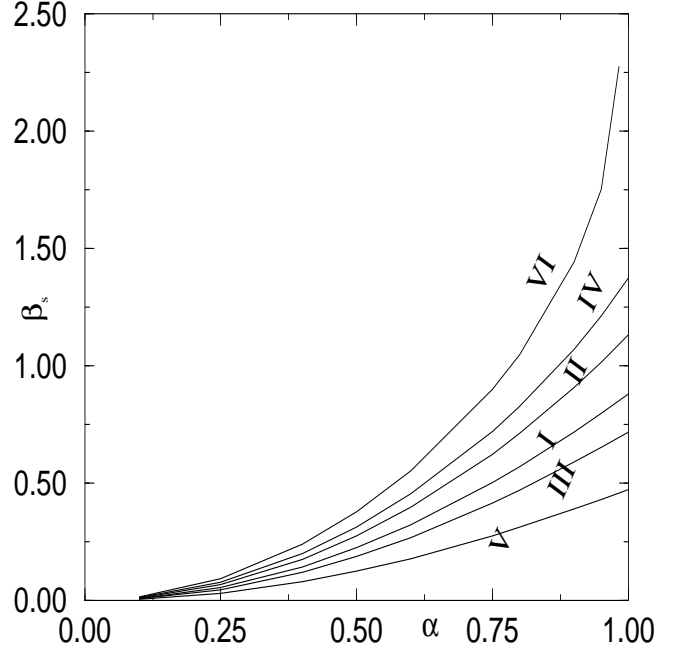


FIG. 7: This figure compares the variation of the smaller root, β_s of Eq.(3.11) for both unstaggered ($\lambda = 1$) and staggered ($\lambda = -1$) stationary localized states as a function of the parameter, α for various values of the nonintegrability parameter, ν . Curve I : $\nu\lambda = -0.1$, Curve II : $\nu\lambda = 0.1$, Curve III : $\nu\lambda = -0.25$, Curve IV : $\nu\lambda = 0.25$, Curve V : $\nu\lambda = -0.5$, and Curve VI : $\nu\lambda = 0.5$.

see that \tilde{H}_0 (Eq.(2.7)) is also a constant of motion. So, we reformulate in this section our variational problem in which, \tilde{H}_0 , in lieu of $\tilde{\mathcal{N}}$ is taken to be the number constant. In this modified variational approach, we take $\tilde{F} = \Lambda_2 \tilde{H}_0 + 2\nu \tilde{\mathcal{N}}$, where $(\Lambda_2 - 1)$ is the Lagrange multiplier. This modified approach also yields Eq.(2.12) for the eigenvalue, ω in Eq.(2.5). One other equation required to solve for one of the two unknowns, namely β and Ψ is given by Eq.(2.13). These results are also derived in Appendix A. From Eq.(2.22) we find that

$$\Psi(\beta, \nu, \lambda, x_0) = a f_1(\beta, \nu, \lambda, x_0) \quad (4.1)$$

where a is a number constant, yields $\tilde{H}_0 = -4\lambda a$, which is again a number constant. Most importantly, in this formulation Ψ is determined explicitly in terms of β within a multiplicative number constant, a . Inasmuch as Ψ is positive semi-definite by definition, the sign of this constant should be such that $a f_1$ is positive semi-definite. Furthermore, in this approach Eq.(2.22) yields $\frac{d\tilde{H}_0}{d\beta} = 0$, irrespective of β . This in turn gives

$$\frac{d\Psi}{d\beta} = - \frac{\frac{\partial \tilde{H}_0}{\partial \beta}}{\frac{\partial \tilde{H}_0}{\partial \Psi}} = \Psi \frac{\partial \ln f_1(\beta, \nu, \lambda, x_0)}{\partial \beta}, \quad (4.2)$$

where we have used Eqs.(2.23) and (2.24). Eq.(4.2) can also be obtained from Eq.(4.1). Now introducing Eq.(4.2) in Eq.(2.13), we get $\frac{d\tilde{N}}{d\beta} = 0$. In other words, permissible values of β are determined from the extrema of \tilde{N} , as a function of β . The determination of extrema in turn needs Eq.(4.2), Eqs.(2.20) and (2.26).

Before we proceed further, we observe the following. Here, we have a variation problem involving two variables, Ψ and β . When Ψ is expressed as a function of β , we obtain the Hamiltonian, $\tilde{H} = \tilde{H}(\beta)$, and SLSs are determined from its extrema, which are obtained by setting $\frac{d\tilde{H}}{d\beta} = 0$. Of course, in stead of β , we could have used Ψ as the fundamental variable. Now, when \tilde{N} is constant, the structure of \tilde{H} (Eq.(2.7)) is such that its extrema are determined from the extrema of \tilde{H}_0 . We have already investigated here this part. On the other hand, we also have the option to take \tilde{H}_0 constant, as it is done in this sections and in sections to follow. In this limit the extrema of \tilde{H} are determined from the extrema of \tilde{N} , provided $\tilde{N}(\beta)$ has extrema. Another equivalent way of envisioning the problem comes from Eq.(2.13), which is, of course the direct consequence of the structure of the Hamiltonian, \tilde{H} (Eq.(2.2)). We can think of an effective dynamical system, having two conjugate dynamical variables, β and Ψ . Then, the Poisson bracket formula, Eq.(2.13) suggests that the effective or the reduced dynamical system can be described by the Hamiltonian, $\tilde{H}_0(\Psi, \beta)$ having a constant of motion, $\tilde{N}(\Psi, \beta)$, or vice versa. Stationary localized states in this dynamical system picture are determined by fixed points (FPs) of the effective or the reduced dynamical system. The two sets of extrema, obtained from two procedures or two pictures may not be identical. So, in the following section, I investigate this aspect of the problem.

A. Equation for the fixed points of the reduced dynamical system and results

Now, if we altogether ignore the infinite sum in Eq.(2.25) which defines $\tilde{N}(\Psi, \beta, x_0)$, we obtain

$$\sqrt{\Psi} = \sinh\left[\frac{\beta}{\sqrt{\Psi(1+\Psi)}} \frac{d\Psi}{d\beta}\right]. \quad (4.3)$$

Introducing Eqs.(4.1) and (4.2) in Eq.(4.3), we get the equation which determines β . If we are mostly interested in the roots of Eq.(4.3), having magnitude less than unit magnitude, we can as before ignore altogether the infinite sum in Eq.(2.21), which defines $f_1(\beta, \nu, \lambda, x_0)$. This further simplifies the equation, which determines β .

When $\nu = 0$, using Eqs.(2.21) and (4.1) we find that $\beta_s = \text{arcsinh } a$ makes the Eq.(4.3) an identity. We shall later show that even with the full expression of $\frac{d\tilde{N}}{d\beta}$, derivable from Eq.(2.25), the above choice of β_s makes $\frac{d\tilde{N}}{d\beta}$ identically zero. In other words, irrespective of \tilde{N}

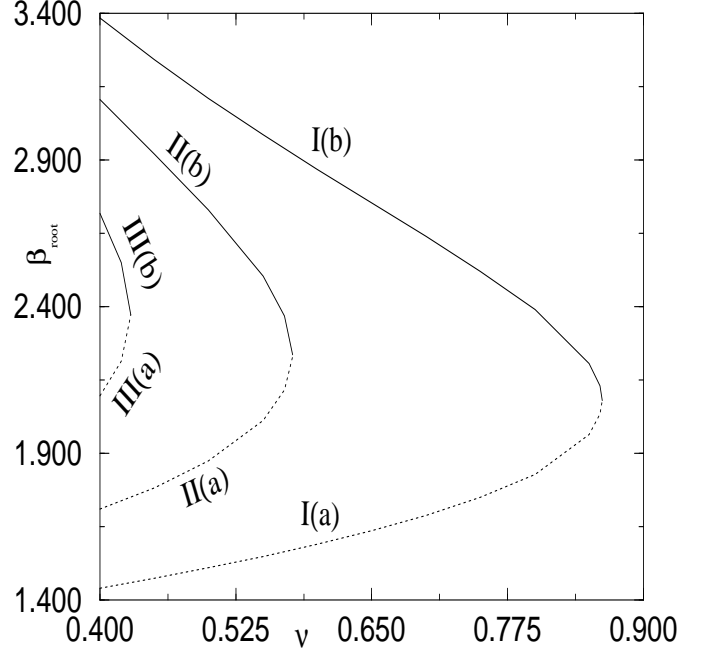


FIG. 8: This figure shows two real roots of Eq.(4.3) in the text as a function of the nonintegrability parameter, ν for three values of the parameter, a . Since, $\lambda = 1$, these states are unstaggered stationary localized states. Curves I(a), I(b) : $a = 1.5$, Curves II(a) and II(b) : $a = 1.75$, and Curves III(a) and III(b) $a = 2.0$. While (a) or the lower part of all curves is for the smaller root, β_s , (b) part or the upper part of these curves show the variation of the larger root β_l . Note that this figure also shows the variation of ν_{critical} as a function of the parameter, a .

or \tilde{H}_0 is taken to be a constant in this constrained variational approach, we get the same stationary AL solitons with $\omega = -2\lambda \cosh \beta$ in both cases. Furthermore, when $\nu \sim o(1)$, we expect from this result that $\beta_s \sim \text{arcsinh } a$. This is also borne out in our numerical calculation, albeit not shown here. We shall show it in the exact calculation.

Considering Eq.(4.3), we consider first the unstaggered localized states with $\nu > 0$. First of all, for every value of $a > 0$, we find a ν_{critical} , such that for $\nu > \nu_{\text{critical}}$, Eq.(4.3) has no real root. On the other hand, $\nu < \nu_{\text{critical}}(a)$, we find two roots of Eq.(4.3) for a given value of $a > 0$. It is also found that β_s is a monotonically increasing function of ν while β_l is a monotonically decreasing function of ν . These features of the solutions are shown in Fig.8. Then, according to our previous discussion, stationary localized states characterized by β_s are stable, while the states characterized by β_l are unstable. In case of staggered localized states having $\nu > 0$, we find that for $|\nu\lambda| > 1$, Eq.(4.3) has no root. Furthermore, $0 < |\nu\lambda| < 1$, Eq.(4.3) has only one root, β_s . We find for $\lambda = -1$, β_s decreases with increasing ν . This is shown in Fig.9. Since, β_s^{-1} gives a measure of the width

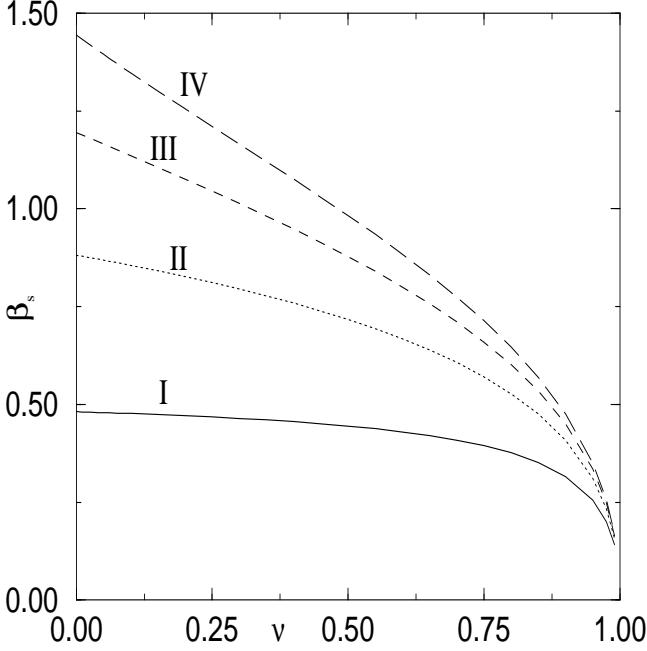


FIG. 9: This figure shows the variation of the smaller root, β_s of Eq.(4.3) in the text as a function of the nonintegrability parameter, ν for various values of the parameter, a . Since, $\lambda = -1$, these states are staggered stationary localized states. Curve I : $a = 0.5$, Curve II : $a = 1.0$, Curve III : $a = 1.5$, and Curve IV : $a = 2.0$.

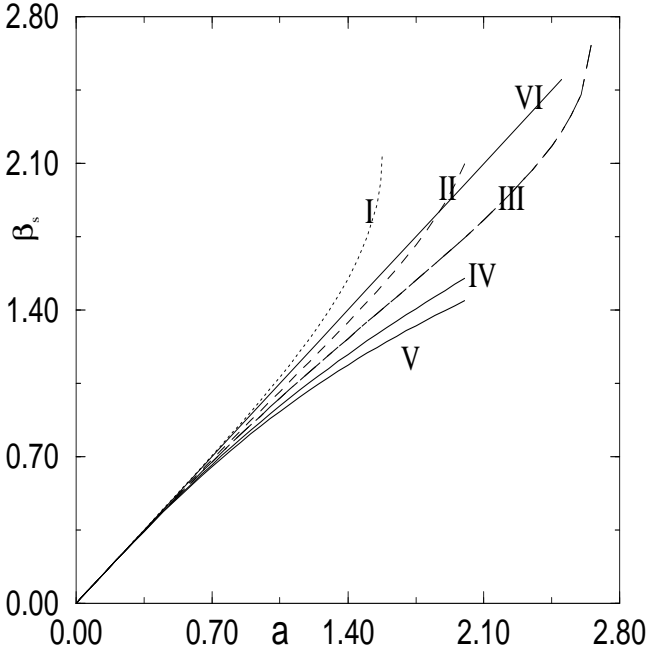


FIG. 10: This figure shows the variation of the smaller root, β_s of Eq.(4.3) in the text as a function of the parameter, a for various values of the nonintegrability parameter, ν . Since, $\lambda = 1$, these states are unstaggered stationary localized states. Curve I : $\nu = 0.75$, Curve II : $\nu = 0.40$, Curve III : $\nu = 0.25$, Curve IV : $\nu = 0.0$. Curve VI is the straight line, $\beta_s = a$.

of the localized states, from our finding we conclude that staggered stationary localized states vanish whenever $|\nu\lambda| \geq 1$. This happens due to effectively repulsive on-site nonlinear potential. This potential helps spread the amplitude over the whole sample. We have already mentioned this. It is also found for both unstaggered and staggered cases that for $a \sim o(1)$, $a \sim \sinh \beta_s \sim \beta_s$, and hence, in this asymptotic limit, Eq.(4.1) together with Eq.(2.21) yields $\sqrt{\Psi} \sim \frac{\beta_s}{\sqrt{1.0 + \nu\lambda}}$. Fig.10 shows the result for the unstaggered states with $\nu > 0$. However, the result for staggered localized states is not shown here. This result agrees with the asymptotic result in Ref.(32).

The next important aspect is to study the effect of x_0 on the formation of these states. Another equally important aspect is to examine if unstable localized states that we find in the truncated equations or equivalently in the leading term analysis exist in the exact calculation. We first emphasize that the problem can be solved exactly in this reformulated version. For our numerical analysis, we use the "FindMinimum" program of "MATHEMATICA-version 4". We discuss below the exact solution.

B. The exact solution

We consider first the case of unstaggered stationary localized states for $\nu > 0$ and $x_0 = 0.0$. Fig.11 shows the variation of β_{root} as a function of the parameter, a for various values of the nonintegrability parameter, ν . The corresponding figure to be compared is Fig.10. We note that for $\nu = 0.0$, we obtain from Eq.(4.1) and Eq.(2.21), $\Psi(\beta, 0.0, \lambda, x_0) = a \sinh \beta$. On the other hand, analytically $\Psi(\beta, 0.0, \lambda, x_0) = \sinh^2 \beta$. So, we must have then $a = \sinh \beta_{\text{root}}$. This is clearly obtained in our numerical analysis. As $\nu = 0.0$ for these curves, both the Curve I of Fig.11 and the Curve V of Fig.10 are defined by the equation $\beta_{\text{root}} = \text{arcsinh } a$. We further see in Fig.11 and also in Fig.10 that for small values of a all curves merge simultaneously on the line $\beta_{\text{root}} = a$ and Curve I (Fig.11) or Curve V (Fig.10). This in turn implies that for $a \sim o(1)$, $a \sim \sinh \beta_{\text{root}} \sim \beta_{\text{root}}$. Hence, for on-site peaked unstaggered localized states, $\sqrt{\Psi} \sim \frac{\beta_{\text{root}}}{\sqrt{1.0 + \nu}}$ is the asymptotic result[32]. We further note that in the exact calculation, we do not find any root corresponding to β_l of Eq.(4.3) for any value of a . This conclusion is reached from the following observation in our numerical analysis. In our numerical analysis, we have used N and M number of terms in two infinite sums in Eqs.(2.21) and (2.25) respectively. We find that $\beta_l \rightarrow \infty$ monotonically if both N and $M \rightarrow \infty$, either separately or simultaneously. So, unstable stationary localized states obtained from Eq.(4.3) are spurious and due to the truncation error. Similar argument should hold good for the analysis of Eq.(3.11).

The variation of β_{root} of unstaggered localized states as a function of ν for various values of a from the exact calculation, and this is shown in Fig.12. We see that β_{root} is

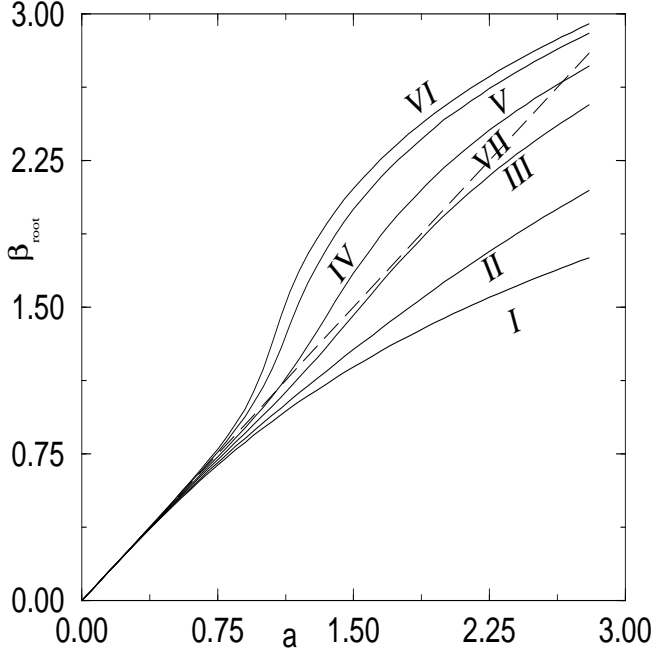


FIG. 11: This figure shows the variation of β_{root} as a function of the parameter, a , for various values of the nonintegrability parameter, ν . This is obtained from the exact calculation. For this figure, $\bar{H}_0 = \text{constant}$, $x_0 = 0.0$, and $\lambda = 1$. Curve I : $\nu = 0.0$, Curve II : $\nu = 0.10$, Curve III : $\nu = 0.40$, Curve IV : $\nu = 0.75$, Curve V : $\nu = 0.90$, and Curve VI : $\nu = 1.0$. Curve VII, the dashed curve is the straight line, $\beta_{\text{root}} = a$.

a monotonically increasing function of ν for $\nu > 0.0$. We note that β_{root}^{-1} gives a measure of the width of the localized states. We have also argued before that the width of the stable unstaggered localized states for this case must decrease with increasing ν . So, $|\beta_{\text{root}}|$ must increase with increasing ν , if it were to characterize stable SLSs. Inasmuch as β_{root} satisfies this criterion, stationary localized states corresponding to β_{root} are stable.

For inter-site peaked unstaggered localized states, having $x_0 = 0.5$, the dependence of β_{root} on a for a fixed ν is also investigated for various values of $\nu > 0$. It is shown in Fig.13. Fig.13 also includes for comparison the variation of β_{root} as a function of a for $x_0 = 0.0$. We note that localized states have larger widths for $x_0 = 0.5$. This, in turn implies that inter-site peaked SLSs will have higher energy. Similarly, the variation of β_{root} as a function of ν for $x_0 = 0.5$, is shown in Fig.14. We again note that stationary localized states for $x_0 = 0.5$ have larger widths. Most importantly inter-site peaked SLSs show weak dependence on ν .

In Fig.15 we show the variation of energy of the on-site and inter-site peaked stationary localized states as a function of ν for $x_0 = 0.0$ and 0.5 . When $\nu \sim o(1)$, the solution approximately has the continuous symmetry of the solution of $\nu = 0.0$ [24, 25]. So, in this limit, both on-

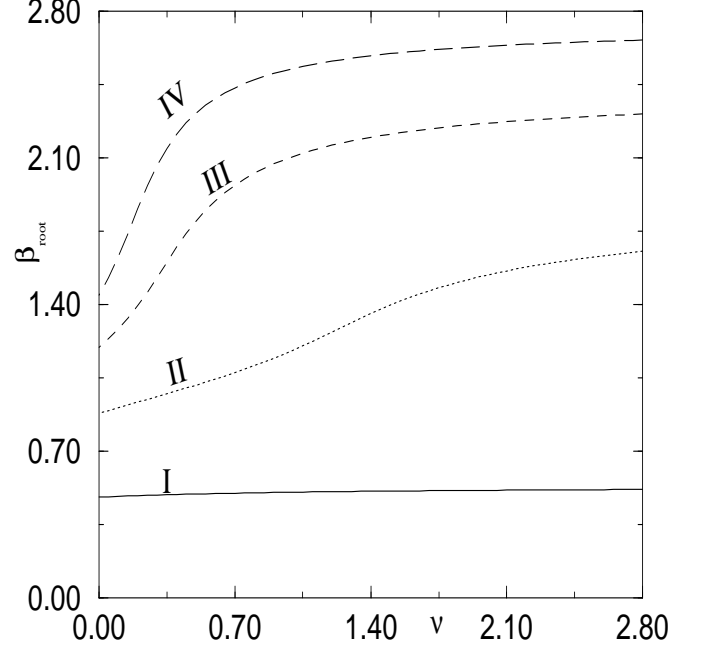


FIG. 12: This figure shows the variation of β_{root} as a function of the nonintegrability parameter, ν for various values of the parameter, a . It is obtained from the exact calculation. For this figure, $\bar{H}_0 = \text{constant}$, $x_0 = 0.0$, and $\lambda = 1$. Curve I : $a = 0.5$, Curve II : $a = 1.0$, Curve III : $a = 1.5$, and Curve IV : $a = 2.0$.

site and inter-site peaked states should have almost the same energy. This is clearly seen in Fig.15. Similarly, on-site peaked states are supposed to be more stable than inter-site peaked states. This is also clearly seen by comparing Curves I(b) and II(b) in this figure. Again, when a reduces, the width of the corresponding stationary localized state increases. Consequently, the energetic distinction between the on-site and inter-site peaked states reduces. This is also clearly evident in Fig.15.

A comprehensive understanding of these results, delineating the basic differences of on-site peaked and inter-site peaked unstaggered SLSs is definitely required. To this end, we note that for $\nu > 0$, these results indicate the operation of a nonlinear attractive potential in the system. This effective nonlinear potential is maximally attractive at lattice sites. From the physical consideration, we argue that the attractive potential assumes minimum values at the center of any two consecutive lattice sites. Since, the system has lattice translational invariance, this potential will also have the periodicity of the underlying lattice. An attractive potential effectively reduces the inter-site hopping of a particle, consequently helping its localization. Secondly, any state can be thought of an effective particle with an effective mass, executing a motion in a potential. From the physical consideration, it is easy to see that stronger is an attractive potential, stronger

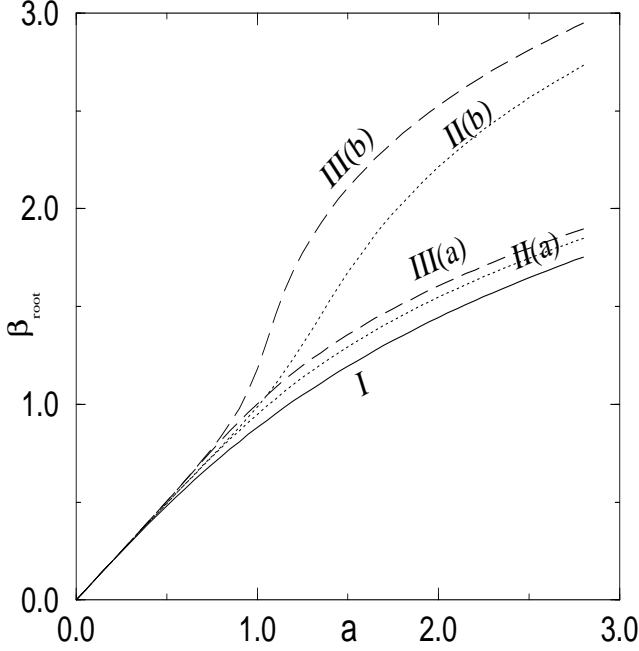


FIG. 13: This figure shows the variation of β_{root} as a function of the parameter, a for two positive values of ν . This figure presents the exact solution for $\lambda = 1$. For the Curve I, $\nu = 0.0$. For Curves II(a) and II(b) $\nu = 0.40$, but $x_0 = 0.5$ and 0.0 respectively. For Curves III(a) and III(b) $\nu = 1.0$, but $x_0 = 0.5$ and 0.0 respectively.

is the localization. Consequently, heavier is the effective mass of the particle. Conversely then the inverse of the effective mass gives the localization length of the effective state. In this picture then the unstaggered SLS for $\nu > 0$ is equivalent to an effective particle sitting either at the bottom of any well ($x_0 = 0.0$) or at the top of the same well ($x_0 = 0.5$). So, the unstaggered SLS with $x_0 = 0.0$ will corresponds to a heavier effective mass particle than the corresponding SLS with $x_0 = 0.5$. In terms of localization length, the first kind of states will be more localized than the second type. Another important deduction from this picture is that energetically, the first kind of states should be more stable. These results are seen in our numerical analysis. Again, when we increase the parameter, a , we increase the maximum amplitude of the SLS. In this effective picture, the depth of the potential well increases. Similar situation also occurs by increasing ν . This, in turn implies that the effective mass of the particle at the bottom of the well will increase with increasing a and ν . So, in both cases, the width of the on-site peaked unstaggered SLS should decrease, as seen in our numerical calculation. The effective periodic potential, however is a function of at least three variables, the position variable, x_0 , the parameter, a and the non-integrability parameter, ν . Since, the SLS with $x_0 = 0.5$ shows weak dependence on ν , our results suggest that

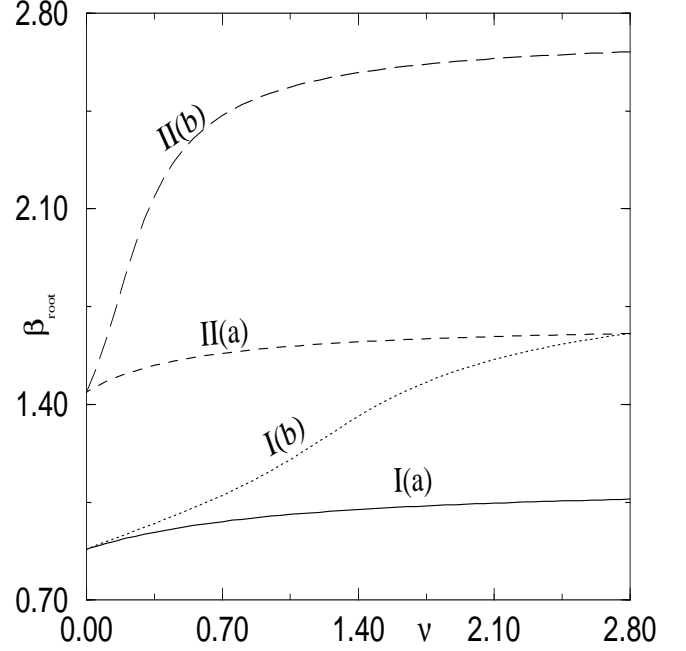


FIG. 14: This figure shows the variation of β_{root} as a function of the nonintegrability parameter, ν for two positive values of the parameter, a . This figure presents the exact solution for $\lambda = 1$. For Curves I(a) and I(b) $a = 1$, but $x_0 = 0.5$ and 0.0 respectively. For Curves II(a) and II(b) $a = 2.0$, but $x_0 = 0.5$ and 0.0 respectively.

the top of the potential is not substantially affected by the change in ν . On the other hand, from our results we deduce that the top of the potential is energetically stabilized by increase in a .

Finally, some exact calculations of β_{root} for staggered SLSs for $\nu > 0$, $\lambda = -1$ and for both $x_0 = 0.0$ and 0.5 are presented. In Fig.16 we present the variation of β_{root} as a function of ν for $a = 1.0$ and 2.0 . Consider first $x_0 = 0.0$. Curves I(a) and II(a) in Fig.16 are almost identical to corresponding curves Fig.9 with a discernible deviation in the magnitude of β_{root} for large values of a together with small values of ν . The same calculation with $\tilde{\mathcal{N}} = \text{constant}$ gives $\beta_s \rightarrow 0$ linearly as $\nu\lambda \rightarrow -1$. See Fig.5. Fig.17 shows the variation of β_{root} as a function of a for various values of $\nu > 0$. The important point to note is that $\beta_{\text{root}}(\nu\lambda < 0) < \beta_{\text{root}}(\nu = 0)$. In other words, SLSs for $\nu > 0$ are stabilized by expansion of the width. As $\beta_{\text{root}} = a$ line becomes tangent to all curves in Fig.17, we infer that when $a \sim o(1)$, $\beta_{\text{root}} \rightarrow a$. Again on the curve $\nu = 0$, $\sinh \beta_{\text{root}} = a$. In this asymptotic limit, we then have from Eqs.(2.21) and (4.1) that $\sqrt{\Psi} \sim \frac{\beta_{\text{root}}}{\sqrt{1-\nu}}$. The corresponding approximate calculation for the model with $\tilde{\mathcal{N}} = \text{constant}$ is shown Fig.6. Fig.6 shows that when $\alpha \sim o(1)$, $\beta_s \sim \alpha^2(1-\nu)$. This in turn yields the same asymptotic result for $\sqrt{\Psi}$. Compar-

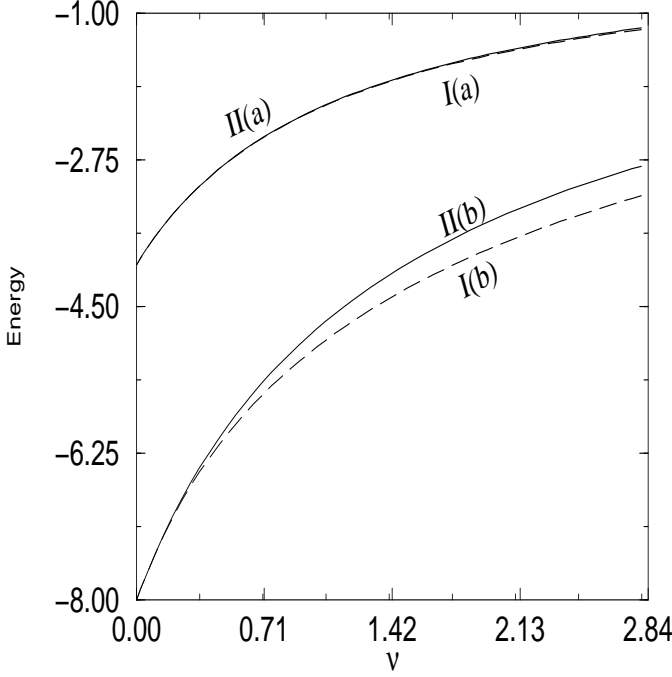


FIG. 15: This figure shows the variation of the energy of unstaggered stationary localized states as a function of ν for two values of a and for two permissible values of x_0 . Of course, the result is obtained from the exact calculation with $\tilde{H}_0 = \text{constant}$. For Curves I(a) and II(a) $a = 1.0$, but $x_0 = 0.0$ and 0.5 respectively. For Curves I(b) and II(b) $a = 2.0$, but $x_0 = 0.0$ and 0.5 respectively.

ing our results for staggered SLSs from three different approaches, namely, approximate calculations with (a) $\tilde{N} = \text{constant}$, (b) $\tilde{H}_0 = \text{constant}$, and (c) the exact calculation with $\tilde{H}_0 = \text{constant}$ and $x_0 = 0.0$, we conclude that all three give qualitatively the same result.

We now consider the basic difference between staggered SLS with $x_0 = 0.0$ and staggered SLS with $x_0 = 0.5$. Fig.16 shows the variation of β_{root} as a function of $\nu \geq 0$ for $a = 1.0$ and 2.0 . From this figure, we see that though $\beta_{\text{root}} \rightarrow 0$ as $\nu \rightarrow 1$ for both $x_0 = 0.0$, and 0.5 , the magnitude of β_{root} for intermediate values of ν is greater for the SLS with $x_0 = 0.5$. This, in turn implies that SLS with $x_0 = 0.5$ has smaller localization length. This is very much opposite to what we observe for an unstaggered SLS. We consider next Fig.18. We define $\Delta E_{lm} = E_l - E_m$, where E_l and E_m define the energy of staggered SLS with $x_0 = 0.0$ and $x_0 = 0.5$ respectively. Fig.18 shows the variation of ΔE_{lm} as a function for $\nu \in [0, 1]$. As $\Delta E_{lm} > 0$ for intermediate values of ν , SLS with $x_0 = 0.5$ is energetically stable compared to its equal counterpart.

In further analysis, we note that the amplitude distribution of staggered SLS around the maximum amplitude site is ST mode like for $x_0 = 0.0$ and P mode like for

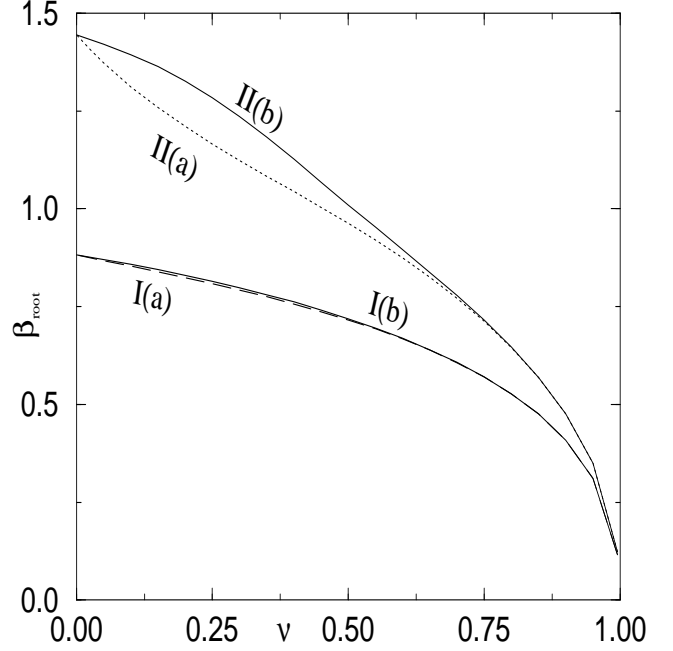


FIG. 16: This figure shows the variation of β_{root} as a function of the nonintegrability parameter, ν for $a = 1.0$ and 2.0 , as obtained from the exact calculation. Since, $\lambda = -1$, these states are staggered stationary localized states. Curve I(a) : $a = 1.0$, and $x_0 = 0.0$. Curve II(a) : $a = 2.0$, and $x_0 = 0.0$. Curve I(b) : $a = 1.0$, and $x_0 = 0.5$. Curve II(b) : $a = 2.0$, and $x_0 = 0.5$.

$x_0 = 0.5$. In this case also there is a periodic arrangement of potential wells in the system. Since, the on-site nonlinear potential is repulsive in this case, this potential will attain the minimum at the center of two consecutive lattice sites. So, the whole periodic arrangement of wells is shifted by half a lattice constant. Consequently, the effective particles corresponding to the P like mode and the ST like mode are sitting at the bottom of a well and at the top of a well respectively[50]. So, the P like mode corresponds to an effective particle with larger effective mass than the corresponding ST like mode, and thereby having a smaller localization length. From this picture, we also deduce that the P like mode is energetically more stable than the ST like mode. Most importantly however, we prove by our variational approach that the existence of P like mode and ST like mode is a fundamental property of a system described by IN-DNLS. To successfully explain the dependence of the localization length of the P like modes on these two parameters, a and ν respectively, we need the following behavior of the potential. When the parameter, a increases, the effective well depth must increase for intermediate values of ν . Consequently, the effective mass of the particle will increase, and the localization length will decrease. But, in case of ν , the effective well depth must decrease as $\nu \rightarrow 1$. Furthermore, as

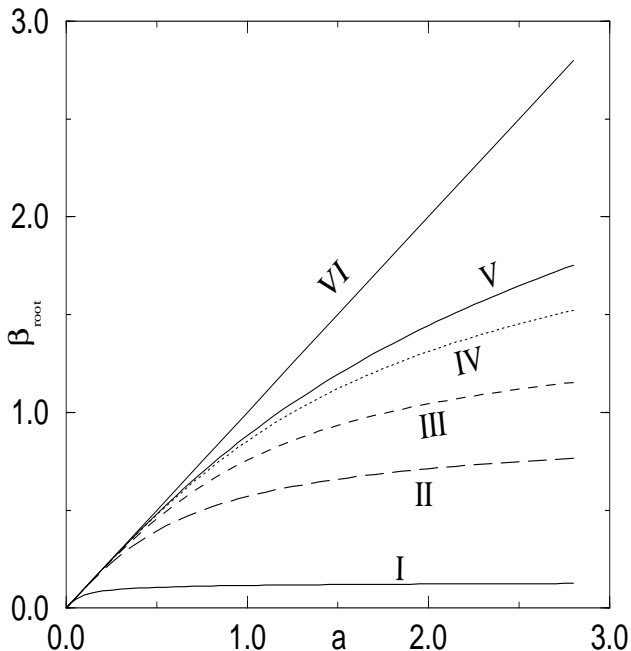


FIG. 17: This figure shows the variation of β_{root} as a function of the parameter, a for positive values of ν . This figure presents the exact solution for $\lambda = -1$ and $x_0 = 0.0$. Curve I : $\nu = 0.995$, Curve II : $\nu = 0.75$, Curve III : $\nu = 0.40$, Curve IV : $\nu = 0.1$, and Curve V : $\nu = 0.0$. Curve VI, the solid curve is the straight line, $\beta_{\text{root}} = a$.

discussed in the context of unstaggered SLS, the dependence of the localization length of ST like modes determines the dependence of the top of the potential well on two important parameters, a and ν .

V. SUMMARY

IN-DNLS is a one dimensional discrete nonlinear equation with a tunable nonintegrability parameter, ν [32, 33]. When $\nu = 0$, it reduces to the famous AL equations[24, 25]. The importance of IN-DNLS in physics as well as in nonlinear mathematics is discussed in the text. In this paper, primarily eigenvalues, energies and corresponding site-amplitudes of SLSs of IN-DNLS are studied using discrete variational formulation[23, 42, 52]. The standard variational approach starts from the respective Lagrangian to study this type of problem. In this paper, however the appropriate functional is derived using the standard variational procedure for finding eigenvalues of Sturm-Liouville equations[58]. In other words, it is shown here how the effective functional can be derived from the Hamiltonian and constants of motion without the prior knowledge of the Lagrangian. The uniqueness of the functional is also established by showing its equivalence to the effective Lagrangian.

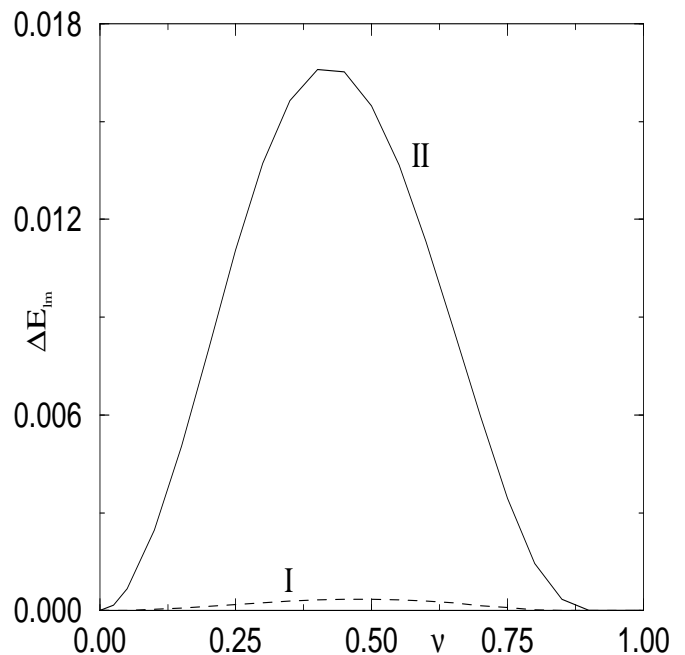


FIG. 18: $\Delta E_{lm} = E_l - E_m$, where E_l and E_m define the energy of staggered SLS with $x_0 = 0.0$ and $x_0 = 0.5$ respectively. This figure shows the variation of ΔE_{lm} as a function for $\nu \in [0.1]$. Curve I : $a = 1.0$, and Curve II : $a = 2.0$.

Inasmuch as localized states in one dimensional linear impure as well as disordered systems show asymptotic exponential decay[37, 38], a "sech" ansatz with two parameters, β and $\Phi = \sqrt{\Psi}$ is used to find eigenvalues and eigenfunctions. In this choice, β^{-1} and $\sqrt{\Psi}$ define the width and the maximum amplitude of SLS respectively. This ansatz is so chosen as it gives AL stationary localized states when $\nu \rightarrow 0$. Furthermore, SLSs of IN-DNLS are assumed to belong to the class of breathers with a single frequency[12]. Since, stationary solitons of AL equations are breathers of this class, this choice of form for SLSs of IN-DNLS is justified.

Very naturally two procedures have emanated in our variational calculation. In the first case, the reduced dynamical system is described by the Hamiltonian, \tilde{H}_0 and $\tilde{\mathcal{N}}$ is taken to be the number constant. In the second case, $\tilde{\mathcal{N}}$ acts as the Hamiltonian. Since, the analysis involves two infinite sums, both sums are ignored in both cases in the leading term analysis. In both cases, for unstaggered stationary localized states two permissible values, namely β_s and β_l of the width parameter, β , are found. It is further found that for two real roots to exist we need $\nu < \nu_{\text{critical}}$ if $\nu > 0$. Furthermore, ν_{critical} is found to be a monotonically decreasing function of the parameter, α , in the first case and a in the second case. These parameters are defined in the text and are positive semidefinite. It is successfully argued from our numeri-

cal analysis that SLSs, characterized by the smaller width parameter, β_s are stable and states characterized by β_l are unstable. However, for staggered SLSs both procedures have yielded a single value, β_s and our numerical results indicate that these are stable localized modes of the system. Though both procedures yield qualitatively same results for the parameters of SLSs, no quantitative comparison is attempted here. Again, it is found that the problem can be exactly solved in the second case. In our exact solution no unstable SLS is obtained. So, the occurrence of unstable SLSs in this system in the leading term analysis should be attributed to the truncation error. In the context of SLS in one dimensional nonlinear systems, this is indeed an important result.

The formation of unstaggered and staggered SLSs are investigated here for $\nu \geq 0$. For the null value of ν , the present variational procedure correctly produces SLSs of AL equation. Furthermore, when $\nu \rightarrow 0$, it is found that $\beta_s \rightarrow \alpha^2$ in the first case for both unstaggered and staggered SLSs. Consequently, AL stationary soliton is recovered in this asymptotic limit. In the second case, $a \rightarrow \sinh \beta_s$ asymptotically as $\nu \rightarrow 0$ in the leading term analysis. This result is true for both unstaggered and staggered SLSs. The same asymptotic results are found in the exact analysis too, except that β_s is replaced by β_{root} . So, in the second case too the AL stationary soliton is the asymptotic result for $\nu \rightarrow 0$. Analytically also the same asymptotic result is obtained here. Our both analytical and numerical results are expected on physical consideration.

In the other asymptotic analysis, $\alpha \rightarrow 0$ in the first case and $a \rightarrow 0$ in the second case. Again, in the second case there are two scenarios, the leading term analysis and the exact calculation. For all cases and for both unstaggered and staggered localized states, the known asymptotic form of Ψ for the stable SLS are obtained numerically from the present variational analysis. This is, therefore a very important contribution of the present work. For unstaggered SLSs, it is found that the width of the state decreases with increasing ν . On the other hand, for staggered SLSs, the width increases with increasing ν and vanishes as $\nu \rightarrow 1$. These results are consistent with the physics of the problem and reasons are given in the text.

Another important aspect is the dependence of the width of SLSs on the position of the maximum amplitude, denoted by x_0 . It is proved in the text that $x_0 = 0$ or $\pm \frac{1}{2}$. It is observed in our analysis that for unstaggered SLSs the on-site peaked SLS ($x_0 = 0$) has smaller width than the inter-site peaked ($x_0 = \pm \frac{1}{2}$) SLS for a given value $\nu > 0$ and $a > 0$. Our analysis also shows that for a given ν and a , the on-site peaked unstaggered SLS is energetically more stable than the corresponding inter-site peaked SLS. These results are physically realistic and are

successfully explained using the effective mass picture. It is found in our analysis that the existence of the P like mode and the ST like mode is a fundamental property of the system, described by IN-DNLS. It is also shown in this numeraoanalytical method that the P like mode is energetically more stable than the corresponding ST like mode. These results constitute a very important contribution of the present work.

It is definitely important to find exact eigenvalues and eigenvectors of the problem. Present analysis may turn out to be a useful guide for the exact calculation. In this analysis we have not proved that the lowest eigenvalue is obtained. Furthermore, the system may have more than one SLS type of ILM. These questions need to be properly investigated. Presence of impurity in the nonintegrability parameter, ν may produce more stationary localized states and these states may interact through further external perturbation. A study of this type is important in the transport in nonlinear systems[19, 21]. In our calculation, we find both P like mode and ST like mode. It will be interesting to know the asymptotic form of these modes in this model. Furthermore, the behavior of these modes under external perturbation should also be investigated. Finally, it is important to find more physical as well as biological systems, where IN-DNLS can be used to study transport properties. A good candidate in this regard is the transport across biological membranes of protons through proton-wires.

APPENDIX A: THE FORMULATION OF DISCRETE VARIATIONAL APPROACH FOR IN-DNLS

We are dealing with a nonlinear eigenvalue problem in our aim to find stationary localized states of IN-DNLS equation, Eqs.(2.2) and (2.5) in the text. For this purpose we are employing variational formulation[23, 53, 58]. To implement the variational approach for this problem, we require the proper functional, \tilde{F} whose constrained variation will lead to Eq.(2.5)[58]. We, of course know a constant of motion and the Hamiltonian, $\tilde{\mathcal{N}}$, and \tilde{H} respectively for the problem at hand[32].

Inasmuch as we know $\tilde{\mathcal{N}}$, and \tilde{H} , using the analogous variational approach of finding eigenvalues in standard Sturm-Liouville problems[58], we set up the functional, $\tilde{F} = \tilde{H} - \Lambda \tilde{\mathcal{N}}$ where Λ is the Lagrange multiplier[59]. We then have for the variation of \tilde{F} , $\delta \tilde{F} = \delta \tilde{H} - \Lambda \delta \tilde{\mathcal{N}}$. For the calculation of the variation, we transform $\Psi_n \rightarrow \Psi_n + \delta \Psi_n$, $n \in Z$ in the expression of \tilde{H} and $\tilde{\mathcal{N}}$ (Eqs.(2.6) and (2.7) respectively) to obtain

$$\begin{aligned}
\delta \tilde{F} &= \delta \tilde{H} - \Lambda \delta \tilde{N} \\
&= -2 \sum_n \frac{\lambda (1 + \Psi_n^2)(\Psi_{n+1} + \Psi_{n-1}) + 2\nu \Psi_n^3 + \Lambda \Psi_n}{1 + \Psi_n^2} \delta \Psi_n.
\end{aligned} \tag{A1}$$

Since, $\{\delta \Psi_n\}$ are arbitrary, $\delta \tilde{F} = 0$ implies that

$$\lambda (1 + \Psi_n^2)(\Psi_{n+1} + \Psi_{n-1}) + 2\nu \Psi_n^3 + \Lambda \Psi_n = 0. \tag{A2}$$

We note that (A.2) is identical to Eq.(2.5) when $\Lambda = \omega$. From further analysis, we find that ω is given by Eq.(2.12) in the text.

For the case, where $\tilde{H}_0 = \text{constant}$, the corresponding functional, \tilde{F} should be given by $\tilde{F} = \Lambda_2 \tilde{H}_0 + 2\nu \tilde{N}$, where $(\Lambda_2 - 1)$ is the Lagrange multiplier. The same procedure will yield Eq.(2.5) if $\Lambda_2 = \frac{2\nu}{2\nu - \omega}$.

So, it is important to note that we can devise the re-

quired functional to determine the eigenvalues of SLSSs by variational approach without the formal knowledge of the Lagrangian.

APPENDIX B: CALCULATION OF THE FUNCTION, $\tilde{N}(\Psi, \beta, x_0)$, EQ.(2.25)

Before we proceed in this section, we cite some results required for the calculation[61].

$$I(s, \Psi, \beta) = \int_0^\infty dy \frac{\cos \frac{\pi s}{\beta} y}{\cosh y + (1 + 2\Psi)} = \frac{\pi \sin \left\{ \frac{2\pi s}{\beta} \operatorname{arcsinh} \sqrt{\Psi} \right\}}{2 \sqrt{\Psi} (1 + \Psi) \sinh \frac{\pi^2 s}{\beta}}. \tag{B1}$$

From (B1) we get

$$\lim_{s \rightarrow 0} I(s, \Psi, \beta) = \frac{\operatorname{arcsinh} \sqrt{\Psi}}{\sqrt{\Psi} (1 + \Psi)} = \frac{d (\operatorname{arcsinh} \sqrt{\Psi})^2}{d \Psi}. \tag{B2}$$

In our calculation, we are using the following ansatz.

$$\Psi_n = \Phi \frac{1}{\cosh \beta(n - x_0)}, \quad n \in Z. \tag{B3}$$

This ansatz has also been used in the previous analysis[32]. For on-site peaked and ST like localized states, $x_0 = 0$, and for inter-site peaked and P like states, $x_0 = \pm \frac{1}{2}$ [23, 45, 46, 47]. We further write $\Phi^2 = \Psi$. The function, $\tilde{N}(\Psi, \beta, x_0)$ is given by Eq.(2.6) in the text. Now introducing (B3) in Eq.(2.6) and then taking partial derivative with respect to Ψ , we get

$$\frac{\partial \tilde{N}}{\partial \Psi} = \sum_{n=-\infty}^{\infty} \frac{1}{\cosh^2 \beta(n - x_0) + \Psi} \tag{B4}$$

We use next the famous Poisson's sum formula, Eq.(2.17) in the text in (B4)[43]. Thereafter, some simple algebraic manipulations are done to obtain

$$\frac{\partial \tilde{N}}{\partial \Psi} = \frac{2}{\beta} I(0, \Psi, \beta) + \frac{4}{\beta} \sum_{s=1}^{\infty} \cos(2\pi s x_0) I(s, \Psi, \beta). \tag{B5}$$

We note that (B5) is identical to Eq.(2.20) in the text. Furthermore, we have from the definition that $\tilde{N}(0, \beta, x_0) = 0$. See Eq.(2.6) in the text. After integration of (B5) over $\Psi' \in (0, \Psi)$ we get Eq.(2.25) in the text. When $\Psi = \sinh^2 n\beta$, $n \in Z$ in Eq.(2.25), we get $\tilde{N}(\Psi, \beta, x_0) = 2n^2\beta$. See Eq.(3.1) in this context. This particular result has been obtained by another route in the literature[17, 36]. We consider now $\nu = 0$ or the AL equation. Then from Eqs.(2.13), (2.20), (2.23), (2.24) and (2.26) we get for $n \in Z$

$$\tanh n\beta \coth \beta - n = 0. \tag{B6}$$

We see then that if $n > 1$, (B6) has no real nonzero β as a solution.

APPENDIX C: APPLICATION OF THE METHOD OF SUCCESSIVE SUBSTITUTIONS IN THE INVESTIGATION OF THE FORMATION OF STATIONARY LOCALIZED STATES IN IN-DNLS

Following the text, we take $\tilde{N}(\Psi, \beta, x_0) = 2\alpha^2 = \text{Constant}$. We further write Eq.(2.25) in the form $\Psi =$

$F(\Psi)$ where the function $F(\Psi)$ is defined as

$$F(\Psi) = \sinh^2[\sqrt{\alpha^2 \beta - f_2(\beta, x_0, \Psi)}], \quad (C1)$$

and in (C1)

$$f_2(\beta, x_0, \Psi) = 2\beta \cos[2\pi x_0] \frac{\sin^2(\frac{\pi}{\beta} \operatorname{arcsinh} \sqrt{\Psi})}{\sinh \frac{\pi^2}{\beta}}.$$

It should be noted that only the first term in the sum in Eq.(2.25) is retained to obtain (C1). To obtain roots of the equation, $\Psi = F(\Psi)$, we can use the method of *successive substitutions*. In this method at the k -th iteration, we write $\Psi_{k+1} = F(\Psi_k)$ with the assumption that $\lim_{k \rightarrow \infty} \Psi_k \rightarrow \Psi_{root}$. However, the necessary condition for this to happen is that $|F'(\Psi_{root})| < 1$ [60]. To explain the use of this method in the calculation,

we shall restrict ourselves only to the first iteration with $\Psi_0 = \sinh^2 \alpha \sqrt{\beta}$. This in turn implies

$$\Psi \sim \Psi_1 = \sinh^2[\sqrt{\alpha^2 \beta - f_2(\beta, x_0, \Psi_0)}]. \quad (C2)$$

Note that in the calculation of roots (Eq.(3.11) in the text) we have taken $f_2 = 0$. By approximating Ψ by Ψ_1 and furthermore keeping only the first term in the sum in the definition of $f_1(\beta, \nu, \lambda, x_0)$ (Eq. (2.21)) we get from Eq.(2.22)

$$\tilde{H}_0 = -4\lambda \frac{\Psi_1}{\sinh \beta} - 4\lambda \nu \frac{\Psi_1}{\beta} [1 + 2\cos 2\pi x_0 \frac{\frac{\pi^2}{\beta}}{\sinh \frac{\pi^2}{\beta}}]. \quad (C3)$$

We then get the permissible values of β by setting $\frac{d\tilde{H}_0}{d\beta} = 0$.

-
- [1] See e.g. Physica D **119**, a special issue on discrete breathers, edited by S. Flach and R. S. MacKay.
 - [2] G. P. Tsironis and S. Aubry, Phys. Rev. Lett. **77**, 5225 (1996).
 - [3] M. Peyrard and A. R. Bishop, Phys. Rev. Lett. **62**, 2755 (1989); A. Campa and A. Giasanti, Phys. Rev. E **82**, 3585 (1998).
 - [4] B. L. Swanson *et al*, Phys. Rev. Lett. **82**, 3288 (1999).
 - [5] J. Kutz, C. Hile, W. Kath, R-D Li, and P. Kummar, J. Opt. Soc. Am B **11**, 2112(1994); H. S. Eisenberg, Y. Silberberg, R. Morandotti, A. R. Boyd and J. S. Aitchison, Phys. Rev. Lett. **81**, 3383 (1998).
 - [6] A. Trombettoni and A. Smerzi, Phys. Rev. Lett. **11**, 2353(2001).
 - [7] P. G. Drazin and R. S. Johnson, *Solitons : an introduction* (Cambridge Univ. Press, Cambridge, 1989).
 - [8] A. Scott, *Nonlinear Science : Emergence & Dynamics of Coherent Structures*, (Oxford University Press, U. K. 1999).
 - [9] R. Z. Sagdeev, S. S. Meiseev, A. V. Tur and V. V. Yanevskii, *Nonlinear Phenomena in Plasma Physics and Hydrodynamics*, ed. R. Z. Sagdeev, (Mir Publishers, Moscow), 137 (1986).
 - [10] V. E. Zakharov and A. B. Shabat, Zh. Eksp. Teor. Fiz. **61**, 118 (1971)[Sov. Phys. JETP **34**, 62 (1972)].
 - [11] S. Flach, K. Kladko, and R. MacKay, Phys. Rev. Lett. **78**, 1207 (1997).
 - [12] S. Flach and C. R. Willis, Phys. Rep. **295**, 181 (1998).
 - [13] R. S. Mackay and S. Aubry, Nonlinearity **7**, 1623(1994); J. L. Marín and S. Aubry, Nonlinearity **9**, 1501(1996).
 - [14] J. L. Marín, S. Aubry and L. M. Floría, Physica D **113**, 283 (1998).
 - [15] K. A. Rasmussen, S. Aubry, A. R. Bishop, and G. P. Tsironis, Eur. Phys. J. B **15**, 169 (2000).
 - [16] J. M. Khatack, Y. Zolotaryuk and P. L. Christiansen, Chaos, **13**, 683 (2003).
 - [17] D. A. Cai, A. R. Bishop and N. Grønbech-Jensen, Phys. Rev. E **52**, R5784 (1995).
 - [18] D. A. Cai, A. R. Bishop and N. Grønbech-Jensen, Phys. Rev. E **52**, 1202 (1996).
 - [19] S. Aubry and T. Cretegny, Physica D **119**, 34 (1998).
 - [20] O. Bang and M. Peyrard Phys. Rev. E **53**, 4143.
 - [21] G. Kopidakis, S. Aubry and G. P. Tsironis, Phys. Rev. Lett. **87**, 165501 (2001).
 - [22] O. M. Braun, and Yu. S. Kivshar, Phys. Rep. **306**, 1 (1998).
 - [23] A. B. Aceves, C. De Angelis, T. Peschel, R. Muschall, F. Lederer, S. Trillo and S. Wabnitz, Phys. Rev. E **53**, 1172 (1996).
 - [24] M. J. Ablowitz and P. A. Clarkson, *Solitons, Nonlinear Evolution Equations and Inverse Scattering* (Cambridge Univ. Press, Cambridge, 1991).
 - [25] M. J. Ablowitz and J. L. Ladik, J. Math. Phys. **16**, 598, (1975), *ibid*, **17**, 1011, (1976).
 - [26] K. Kundu, J. Phys. A. Math. Gen. **35**, 8109 (2002).
 - [27] P. M. Chaikin and T. C. Lubensky, *Principle of condensed matter physics*, (Cambridge University Press, 1998).
 - [28] K. Kundu, Phys. Rev. E, **61**, 5839 (2000).
 - [29] S. V. Dmitriev, Yu. S. Kivshar and T. Shigenari, Phys. Rev. Lett., **64**, 056613 (2001).
 - [30] Y. S. Kivshar and D. K. Campbell, Phys. Rev. E **48**, 3077 (1993).
 - [31] A. A. Vakhnenko and Yu. B. Gaididei, Theo. Math. Fiz. **68**, 350 (1986) [Theor. Math. Phys. **68**, 873 (1987)].
 - [32] D. Cai, A. R. Bishop, and N. Grønbech-Jensen, Phys. Rev. Lett. **72**, 591 (1994).
 - [33] M. Salerno, Phys. Rev. A **46**, 6856 (1992).
 - [34] M. Johansson and Yu. S. Kivshar, Phys. Rev. Lett. **82**, 85 (1999); Yu. S. Kivshar and M. Peyrard, Phys. Rev. A **46**, 3198(1992).
 - [35] P. Marquisé, J. M. Bilbault, and M. Remoissenet, Phys. Rev. E **51**, 6127(1995).
 - [36] D. Cai, A. R. Bishop, and N. Grønbech-Jensen, Phys. Rev. E **53**, 4131 (1996).
 - [37] E. N. Economou, *Green's Functions in Quantum Physics*, (Heidelberg : Springer, 1983).
 - [38] H. Matsuda and K. Ishii, *Suppl. Prog. Theo. Phys.* **45**, 56 (1970); K. Ishii *Suppl. Prog. Theo. Phys.* **53**, 77 (1973).
 - [39] D. H. Dunlap, H-L Wu and P. Phillips, Phys. Rev. Lett.

- 65**, 88 (1990).
- [40] K. Kundu, D. Giri and K. Ray, J. Phys. A : Math Gen. **29**, 5699 (1996).
 - [41] B. C. Gupta and K. Kundu, Phys. Lett. A **235**, 176 (1997); B. C. Gupta and K. Kundu, Phys. Rev. B **55**, 11033 (1997); B. C. Gupta and K. Kundu, Phys. Rev. B **55**, 894 (1997); A. Ghosh, B. C. Gupta and K. Kundu, J. Phys.: Condens. Matter **10**, 2701 (1998).
 - [42] K. Kundu and B. C. Gupta, Eur. Phys. J. B **3**, 23 (1998); B. C. Gupta and K. Kundu, *Nonlinear Dynamics: Integrability and Chaos* Eds. M. Daniel, K. M. Tamizhmani and R. Sahadevan, p. 193 (Narosa, New Delhi, 2002)
 - [43] J. M. Ziman, *Principles of The Theory of Solids*, Second ed., (Cambridge University Press, Cambridge, Great Britain, 1972).
 - [44] Yu. S. Kivshar, F. Zhang and A. S. Kovalev, Phys. Rev. **55**, 1 (1997).
 - [45] A. J. Sievers and S. T. Takeno, Phys. Rev. Lett. **61**, 970(1988).
 - [46] J. B. Page, Phys. Rev. B **41**, 7835(1990).
 - [47] K. W. Sandusky, J. B. Page and K. E. Schmidt, Phys. Rev. B **46**, 6161(1992).
 - [48] S. Darmanyán, A. Kobaykov and F. Lederer, Zh. Éksp. Teor. Fiz. **113**, 1253 (1998) [JETP **86**, 682 (1998)].
 - [49] P. G. Kevrekidis, A. R. Bishop, and K. Ø. Rasmussen, Phys. Rev. E **63** 036603 (2001).
 - [50] Ch. Claude, Y. S. Kivshar, O. Kluth and K. H. Spatchek, Phys. Rev. B **47**, 14228 (1993).
 - [51] S. Takeno, J. Phys. Soc. Jpn. **58**, 759 (1989).
 - [52] B. Malomed and M. L. Weinstein, Phys. Lett. A **220**, 91 (1996).
 - [53] D. Anderson, Phys. Rev. A **27**, 3135 (1983)
 - [54] B. A. Malomed and R. S. Tasgal, Phys. Rev. E **49**, 5787 (1994)
 - [55] D. J. Kaup and T. I. Lakoba, J. Math. Phys. **37**, 3442 (1996).
 - [56] A. Das, *Integrable Models*, (World Scientific, Singapore, 1989).
 - [57] B. A. Malomed and J. Yang, Phys. Lett. A **302**, 163 (2002).
 - [58] F. B. Hildebrand, *Methods of Applied Mathematics*, Second ed., (Prentice-Hall, New Jersey).
 - [59] F. B. Hildebrand, *Advanced Calculus For Applications*, Second ed., (Prentice-Hall, New Jersey, 1976).
 - [60] F. B. Hildebrand, *Introduction To Numerical Analysis*, Second ed., (Dover New York 1974).
 - [61] I. S. Gradshteyn and I. M. Ryzhik, *Table of Integrals, Series and Products*, Fourth ed., (Academic Press, New York, 1980), M. Abramowitz and I. A. Stegun, *Handbook of Mathematical Functions*, Ninth ed., (Dover, New York, 1970).